



MASTER OF BIOMEDICAL ENGINEERING

**Feasibility Design of AI Egen Based Urine Test Strip  
for Early Detection of Chronic Kidney Disease**

**Topic Number and Name:**

ENGR9700 ENGINEERING THESIS PROJECT REPORT

**Semester and Year:**

Semester 2 - 2017 & Semester 1 - 2018

**Name of Student and ID:**

Xinyi Zhang - 2159118

**Name of Supervisor:**

A/Prof. Youhong Tang

**Date of Report Submitted:**

21 / May / 2018

**Grade:**

Submitted to College of Science and Engineering in partial fulfillment of the requirements for the degree of Master of Biomedical Engineering at  
Flinders University - Adelaide Australia

# Table of Contents

<b>Abstract</b> .....	<b>4</b>
<b>Declaration</b> .....	<b>5</b>
<b>Acknowledgements</b> .....	<b>6</b>
<b>Chapter 1: Introduction</b> .....	<b>7</b>
<b>1.1 Background</b> .....	<b>7</b>
1.1.1 Chronic kidney disease (CKD) .....	7
1.1.2 Urine albumin .....	7
1.1.3 Urine albumin detection methods.....	8
<b>1.2 New opportunity for test strip improvement</b> .....	<b>11</b>
1.2.1 Aggregation-induced emission fluorogen (AIEgen).....	11
1.2.2 Albumin specified AIEgen: BSPOTPE .....	13
1.2.3 Method of image processing for testing HSA under liquid state .....	13
<b>1.3 Aims</b> .....	<b>14</b>
<b>1.4 How to achieve the aims</b> .....	<b>14</b>
<b>1.5 Outline of the following chapters</b> .....	<b>15</b>
<b>Chapter 2: Literature Review</b> .....	<b>16</b>
<b>2.1 Strip design based on dip methodology</b> .....	<b>16</b>
<b>2.2 Strip design based on drop methodology</b> .....	<b>18</b>
2.2.1 Configuration of the lateral flow test strip .....	18
2.2.2 Immunochromatographic assay (ICA).....	19
2.2.3 Fluorescent immunochromatographic assay (FICA).....	23
<b>2.3 AIEgen applications</b> .....	<b>26</b>
<b>2.4 AIEgens for health monitoring</b> .....	<b>27</b>
<b>2.5 Current research of BSPOTPE for urine albumin detection</b> .....	<b>28</b>
2.5.1 BSPOTPE characteristics .....	28
2.5.2 Smartphone-based urinalysis using BSPOTPE bioprobe .....	31
<b>Chapter 3: Materials and methods</b> .....	<b>34</b>
<b>3.1 Materials</b> .....	<b>34</b>
3.1.1 Chemicals .....	34
3.1.2 Chemical sample preparation .....	34
3.1.3 Test strip materials .....	35
3.1.4 Test strip configuration .....	36
3.1.5 Other information .....	36
<b>3.2 Methods</b> .....	<b>37</b>
3.2.1 Assay procedure .....	37
3.2.2 Test strip design methodology .....	38
<b>Chapter 4: Results and discussion</b> .....	<b>40</b>
<b>4.1 Strip based on dip method</b> .....	<b>40</b>
4.1.1 Strip design .....	40
4.1.2 Glass fiber .....	41
4.1.3 Reagent concentration optimization .....	44
4.1.4 Incubation time .....	46
4.1.5 Dipping time .....	47
4.1.6 Waiting time .....	48
4.1.7 Result .....	49

<b>4.2 Strip based on drop method</b> .....	<b>51</b>
4.2.1 Strip design .....	51
4.2.2 Nitrocellulose membrane (NC membrane).....	53
4.2.3 Glass fiber .....	57
4.2.4 Testing time.....	58
4.2.5 Result .....	60
<b>4.3 Method comparison</b> .....	<b>62</b>
4.3.1 Dip and drop assay comparison.....	62
4.3.2 Traditional urine test strip comparison .....	63
<b>4.4 Limitations of the research</b> .....	<b>64</b>
<b>4.5 Future directions of further advance study</b> .....	<b>65</b>
4.5.1 Combination with immunoassay .....	65
4.5.2 Advanced material search.....	66
4.5.3 New strip configuration.....	66
4.5.4 Evaluation tool improvement.....	67
<b>Chapter 5: Conclusions</b> .....	<b>68</b>
<b>Appendixes</b> .....	<b>69</b>
<b>Appendix 1: Conference collection</b> .....	<b>69</b>
<b>Appendix 2: MATLAB code</b> .....	<b>70</b>
<b>References</b> .....	<b>73</b>

# Abstract

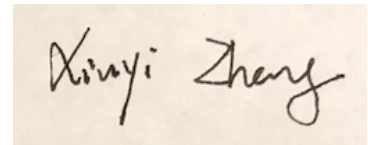
One-third of Australians are at risk of developing chronic kidney disease (CKD). Clinical practice guidelines have recommended that the test for urine albumin should be used to screen for CKD. A healthy kidney does not allow albumin to pass into the urine, but a damaged kidney allows, so early detection of CKD can reduce the kidney failure by up to 50 percent. People normally use micro-albuminuria, which means the protein concentration is 30-300 mg/L, to detect CKD in the early stage. A few in-vitro diagnostic devices are based on fluorescent emission to assay the chronic kidney disease, such as the strip test, also known as the lateral flow assay which always combines a device for quantitative analysis. A strip is composed of four parts and when the sample drops on it, the sample will flow and pass through the various parts to separate into individual components. This is called lateral flow assay and there is a test line in the reaction part. The antibody is labelled with fluorogen, e.g., quantum dot (QD), when the sample passes through, the analyte, which is the antigen will have reaction with antibody in the test line. The fluorogen will be lighted on. We can use the light intensity to quantify the analyte concentration.

The aggregation-induced emission (AIE) effect is a group of fluorogen materials become highly luminescent when they are aggregated in solid state or in poor solvents, which is opposite to the aggregation caused quenching (ACQ) effect, i.e., the effect will cause the QD labelled antibody quench when they aggregate together in the test strip. The AIEgens are successfully used as various bioprobes, such as they can be used as biological probes to detect human serum albumin in urine. Compared with conventional fluorogen systems, the AIEgen based sensing systems have better stability, higher signal-to-noise ratio and lower detection limits, which provides a new opportunity to look into the redevelopment of urine test strip.

In this feasibility study, we try to use a specified designed AIEgen to substitute the expensive, tedious-prepared and ACQ effecting QD fluorogen labelled antibody and the corresponding antigen in the current test strip, and redevelop the test strip to achieve more cost-effective and acceptable detection ability for the in-vitro diagnostic system. The individual parts of the strip, such as sample pad, conjugate pad, NC membrane, and the assembled strip using the optimized individuals have been evaluated with different incubation times and AIEgen concentrations in this research.

# Declaration

I certify that this work does not incorporate without acknowledgment any material previously submitted for a degree or diploma in any university; and that to the best of my knowledge and belief it does not contain any material previously published or written by another person except where due reference is made in the text.

A rectangular image showing a handwritten signature in black ink on a light-colored background. The signature reads "Xinyi Zhang" in a cursive style.

Xinyi Zhang  
21 May 2018

# Acknowledgements

I would like to use this opportunity to express my appreciation to my supervisor Associate Professor Youhong Tang who is abundantly helpful. I am thankful for his aspiring guidance and simulating encouragement during my thesis project. Furthermore, a special gratitude to all project members: Shaymaa Akraa, Tran Tam Anh Pham, and Ravichandran Rasiah. The learning and practicing process of this thesis gives me much pleasure. I have learned academic knowledge and valuable experiences in this field, which supports me to improve my future work. At last, I thank all the teachers and students who help me directly and indirectly. The thesis project helps me obtain confidence and feel more prepared for future academic study.

# Chapter 1: Introduction

## 1.1 Background

### 1.1.1 Chronic kidney disease (CKD)

According to clinical practice guideline developed by the Kidney Disease Improving Global Outcomes (KDIGO) organisation, the chronic kidney disease (CKD) is recognized as disorders of kidney structure or function which presents for over 3 months with implications[1]. Early identification of CKD can highly prevent disease progression and reduce complication risk. However, early stages of CKD are often asymptomatic[2]. When patients realize symptoms, CKD will proceed fast and can be only treated by dialysis and transplantation[2].

CKD identification depends on precisely measuring glomerular filtration rate (GFR) and albuminuria[1]. The albuminuria presents stages of kidney damage. The clinical practice guideline recommends that measurement of albumin concentration should be taken for evaluation of albuminuria[3].

### 1.1.2 Urine albumin

Albumin is the most significant protein lost in CKD patients' urine[3]. The composition of urine albumin molecules is complicated and changes dramatically, therefore it is difficult to measure. Human serum albumin (HSA) is the amplest protein in human body and is synthesized in liver. It is a 585 amino acid protein with molecular weight of 66.5kDa. It has N- and C-terminal truncations, 4 globular domains and 17 disulfide bonds, which could bind to multiple ligands[5].

A healthy kidney filters out waste but keeps albumin. Excess amount of albumin in urine indicates CKD. Micro-albuminuria is defined by concentration of 30-300mg/L HSA in the urine[4]. The micro-albuminuria test is performed as initial screening method for CKD in the early stage.

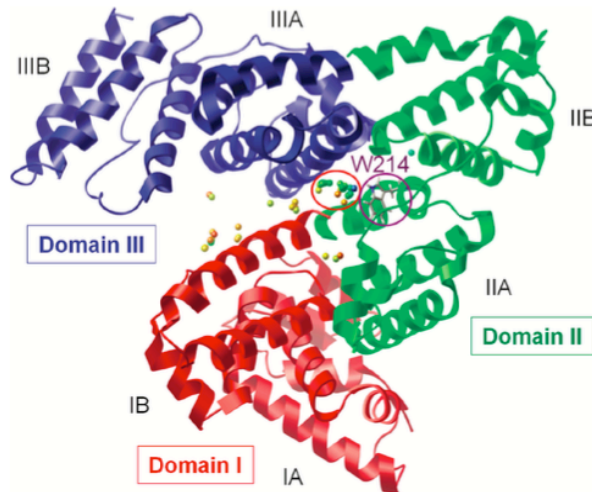


Figure 1. The HSA structure. Different colors present domains of HSA, with red, green, and blue for domains I, II, and III, respectively[4].

### 1.1.3 Urine albumin detection methods

Urine albumin can be assessed both in the central laboratory and at the bedside. The key issue of the measurement is associated with the tradeoff between convenience and precision[6]. Although albumin assay in the clinical laboratory is expensive, the measurement is recommended by guideline because of its advantages[2]. Global routine measurement of urine albumin in professional laboratory are immunoassay-based and immunoturbidimetric, such as radioimmunoassay (RIA), enzyme-linked immunosorbent assay (ELISA), chemiluminescence immunoassay (CLIA), nephelometry and turbidimetry[7]. The detection limit is at 2-10mg/L[8]. According to Martin's review, immunoassay measurement procedures might underestimate albumin considerably[5]. It is hard for antibodies to monitor various forms of albumin[8]. Other alternative methods include high performance liquid chromatography (HPLC), liquid chromatography-mass spectrometry (LC-MS), and liquid chromatography-tandem mass spectrometry (LC-MS/MS)[8]. HPLC enables giving higher detection values of albumin than immunoassays. However, Chen states that this is caused by detection of similar size molecules of other proteins[8]. LC-MS is hard to detect albumin fragments without



N-terminal truncations. LC-MS/MS enables detecting intact albumin and albumin fragments while the detection may be affected by post-translational modifications[8].



Figure 2. RIA test kit and reader[30, 31]



Figure 3. ELISA test kit and reader[32, 33].

Historically, albumin is ascertained easily due to ease of measurement, particularly using urine test strip. Home available test strip for urinalysis enables receiving immediate test results. It is commonly used as initial screening test for CKD. There are two types of test strips used for albumin detection. One is dip strip based on colorimetric method and another is drop strip using lateral flow assay.

The dip strip is mounted with different sensitive chemicals. This approach depends on the color variation of the strip after the chemicals have interaction with urine sample. It is limited in quantitative result due to its low sensitivity and hard discrimination. The albumin concentration resulted from micro-albuminuria cannot be assayed quantitatively by this method[4].



Figure 4. Urine test strips[34].

Another drop strip is normally performed by immunochromatographic assay. The result depends on the correlation between the color intensity of test line and the analyte concentration. Currently, the strip uses colloidal gold nanoparticles or fluorophore as labels to coat antibody. The strip employed colloidal gold nanoparticles only performs qualitative or semi-quantitative analysis. The fluorophore based strip can conduct quantitative analysis. In this study, we focus on fluorophore methodology. The sensitivity and accuracy of this strip rely on the immunoreaction between antibody coated with fluorophore and antigen (analyte). The process to produce this strip is complicated and expensive. Most of the fluorophore is produced as quantum dots (QDs) which are semiconductor particles and only nanometers in size. For the QDs as the fluorescent bioprobe, there is a serious drawback named aggregation-caused quenching (ACQ) effect. The ACQ fluorophore often encounter reducing or quenching in solid state, which leads to reducing the sensitivity of the test[9]. The ACQ effect hinders the development of test strips for on-site detection[10]. The fluorophore level reaches its maximum in solid state because of the absence of solvent, which leads to the ACQ effect becoming severely[11]. This effect limits the scope of application as fluorescent bioprobes in both liquid and solid state. There is no effective method to eliminate the ACQ effect[12].

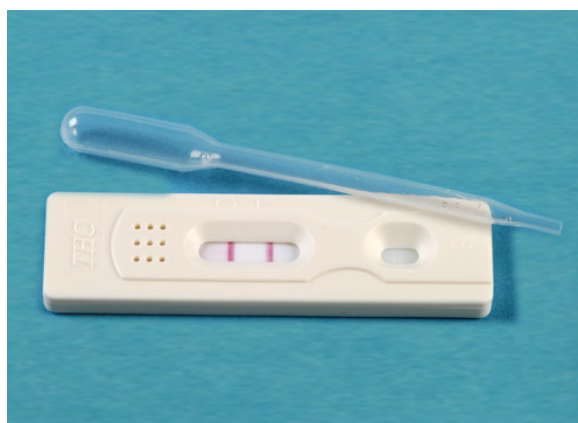


Figure 5. The drop strip based on colloidal gold nanoparticles assay[35].

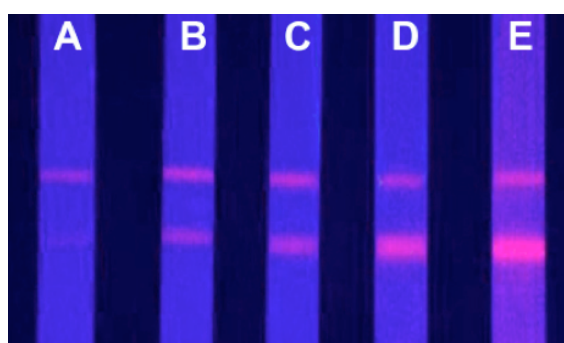


Figure 6. The fluorescence imaging of the drop strip based on QD assay[36].

## 1.2 New opportunity for test strip improvement

### 1.2.1 Aggregation-induced emission fluorogen (AIEgen)

Fluorescent bioprobes have attracted many researches because of good sensitivity, selectivity and rapidity. Many organometallic complexes are produced for protein assay. Through conjugation with proteins, the luminophores enhance their emission and perform spectral shifts. This advantage can support to detect and quantify the biopolymers. However, some of the fluorescent probes are hard to be dissolved in aqueous media; some of them are not stable under ambient conditions. Although several fluorophores present excellent performances in protein assays, they are extremely expensive due to difficult syntheses. These disadvantages restrict the scope of their applications[4].

In 2001, Ben Zhong Tang in the Hong Kong University of Science and Technology discovered that light-emitting process can be constructed but not be destructed by the luminogen aggregation. Some silole molecules can be luminescent in the aggregated

state as films in the solid state however not emissive in the solution state. This novel phenomenon is named 'aggregation-induced emission' (AIE). The non-luminescent silole molecules can be guided to emit light under aggregate formation[10]. The AIE effect is totally on the contrary of the ACQ phenomenon. The AIE effect has practical applications: one can conduct advantages of aggregated formation but not perform against it. It enables the use of any concentration of the dye solution for bioassay and permits the development of biosensors by using luminogen aggregation to light up[10].

The AIE effect results from restriction of intramolecular rotation (RIR) in the aggregates. The researchers have developed various AIE luminogens and figured out their applications as valuable materials such as chemo-sensors, bioprobes and emitter in solid state[10]. It is currently observed in molecules which have rotating units, for instance phenyl rings. The rotor-containing fluorogens experience low frequency motions in solution with low concentration, which leads to fast non-radiative decay of the excited state. This process causes the fluorogens non-emission. In the aggregates, intermolecular steric interaction restricts motions, which encourages to open the radiative pathway[12].

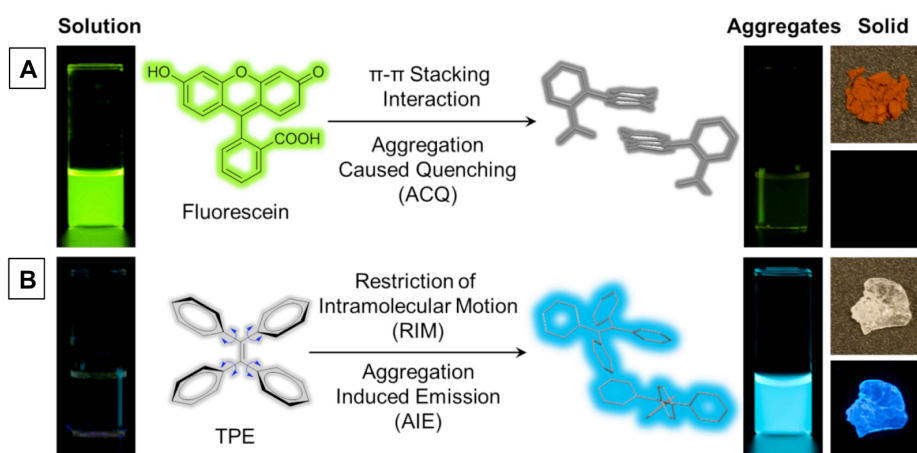


Figure 7. ACQ and AIE effect principles[37].

Another advantage is the conjugation of AIE fluorogens and receptors causes light-up bioprobe for specific analyte monitoring. Compared with the conventional fluorescent light-off bioprobes which are performed by ACQ effect, the light-on feature of the AIE probes provides better sensitivity and accuracy. It helps to visualize the analytes directly and to process in aqueous media. The performance of AIE

bioprobe can be improved by particle formulation and surface functionalization. This new bioprobe shows advanced features in respect of brightness, biocompatibility and cellular retention. The features are better than traditional inorganic QDs and organic dyes[12]. The nano-aggregated AIE bioprobes are organic versions of inorganic QD probes. The QD probes comprise heavy metals and chalcogenic elements. Hence, they are cytotoxic inherently. One advantage is that the AIE nano-bioprobes are less cytotoxic but as sensitive as the inorganic QD probes[10]. The merits of AIE fluorogen provide a new opportunity for monitoring HSA by test strip.

### 1.2.2 Albumin specified AIEgen: BSPOTPE

A new type of AIE fluorogen is examined as bioprobe for detecting and quantifying HSA. It is a TPE salt, sodium 1,2-bis[4-(3-sulfonatopropoxyl)phenyl]-1,2-diphenylethene (BSPOTPE)[4]. The fluorescent light-on property of BSPOTPE through its complexation with albumin encourages the quantitative detection of HSA in the aqueous media and visual observation in the gel electrophoresis. Hong's research examines the feasibility of HSA quantitation in artificial urine. The research presents BSPOTPE has good sensitivity and selectivity to albumin. Because of the AIE property of BSPOTPE, the detection limit is able to be altered by changing the concentration of fluorogen[4]. This result enables to further develop its clinical application, such as urine test strip development[4].



Figure 8. Chemical structure of BSPOTPE [4]

### 1.2.3 Method of image processing for testing HSA under liquid state

A new study presents a development of a smartphone-based urinalysis device, which enables people monitoring reliable quantitative analysis of HSA applying

BSPOTPE bioprobe under liquid state [13]. The study uses a smartphone to capture cuvette images and processes these images by image software. It conducts image processing to model a linear relationship between the luminescent cuvette and the albumin concentration [13]. The researchers choose the HSL (Hue, Saturation, and Lightness) model to transform the visible electromagnetic spectrum (color) into a digital signal. The result shows that a prediction model of albumin concentration with linear correlation is obtained[13]. This study provides a solution of portable albumin detection and proves that the smartphone software has the ability to perform urinalysis and telemedicine by using BSPOTPE bioprobe. However, this method is performed under liquid state which is not hygienic and convenient to real world. Therefore, it is necessary to develop a test strip based on this method using BSOPTPE bioprobe.

### **1.3 Aims**

A feasibility study on designing an AIEgen bioprobe based urine test strip will be conducted for early detection of chronic kidney disease. We will try to find the optimized material of each strip component and to obtain the best test conditions for both dip and drop strip designs. The study will apply image processing software to analyze the image light intensity. After the evaluation of the test, an equation between fluorescent light intensity and albumin concentration will be obtained as well as the detection ranges of both dip and drop methods will be examined. For further development, the comparison of different test strip designs will be investigated.

### **1.4 How to achieve the aims**

To achieve the research aims, we have to indicate the gaps of traditional design and how to fit into these gaps. As previously described, there are two methodologies to design the test strip. The dip method based on colorimetric assay has low sensitivity and accuracy. The drop method based on lateral flow assay and immunoassay is complicated and its QD labels are discouraged by ACQ effect. Our design needs to simplify the strip by applying image analysis software and the new AIEgen bioprobe named BSPOTPE. The new BSPOTPE bioprobe has the selectivity

to albumin and no ACQ effect happened. Therefore, we can use this notable bioprobe to replace conventional reagent and sustain the sensitivity and accuracy of the previous QD labeled strip. The function of each strip's component and the properties of strip's raw material have to be understood deeply. How the albumin is detected quantitatively by BSPOTPE bioprobe and what the optimized test conditions are, also need to be figured out during this study.

## 1.5 Outline of the following chapters

This thesis describes the background knowledge of kidney disease, urine albumin, conventional detection methods, and new opportunities for test strip improvement including notable AIEgen material BSPOTPE and image analysis of fluorescent light intensity by smartphone. Furthermore, it reports literature review of current test strip designs and AIEgen applications. The strip design of this study is based on the methods of dip assay and drop assay. Both methodologies are described in literature review chapter. The AIEgen applications for health monitoring and current research of BSPOTPE are also evaluated from our theoretical perspective. Then the thesis reports the materials and methods of this design study. The result and discussion chapter is presented at last to further demonstrate the feasibility of designing an AIEgen based urine test strip for early detection of chronic kidney disease. Afterwards, the conclusions will be delivered as well.

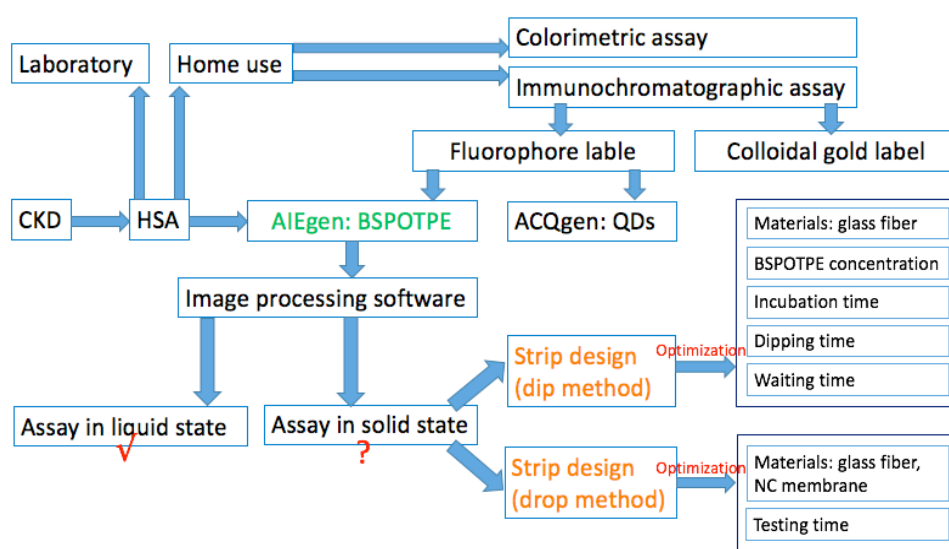


Figure 9. Architecture of the thesis project.



# Chapter 2: Literature Review

## 2.1 Strip design based on dip methodology

The traditional urine test strip for albumin detection is based on principle of the protein error of tetrabromophenol blue. This strip method is moderately sensitive (but not selective) to albumin[14]. The test strip is dipped into the urine sample and extracted out to further distinguish the color variation. It is a semi-quantitative colorimetric method. Albumin result is graded as five levels: trace, 1+, 2+, 3+ and 4+. It uses color difference to determine the albumin levels. When concentration of urine protein increases, one dye indicator, which is tetrabromophenol blue, experiences successive color variation from green to blue. The process of tetrabromophenol blue binding with proteins is pH dependent. Albumin connects to the indicator at pH 5-7 and other proteins connect at pH below 5. The urine pH is normally between 5-6, as a result, urine test strip is specific to albumin essentially[15]. The detection limit of test strip sensitivity is about 150mg/L[8].



Figure 10. Strip design based on dip methodology[38,39].

Early kidney disease is characterized by micro-albuminuria (30-300mg/L) whose lower concentration limit is below the detection limit of the test strip (150mg/L). Thus this colorimetric test cannot detect early kidney disease. Macro-albuminuria means albumin is greater than 300mg/L and only at this concentration the result of urine test strip is positive[15]. A study shows that urine test strip values of >1+ have positive



predictive value of 92% for detecting >300 mg/L[16]. Strip values of negative to trace are not able to figure out notable albuminuria because its negative predictive value is just 34%[16]. False positive and negative results are usual in urinalysis by this strip. Color discrimination on strip can be affected by many reasons[6]. Environmental factors may also influence the strip test. Chemicals on the strip may degrade under light, heat and humidity.

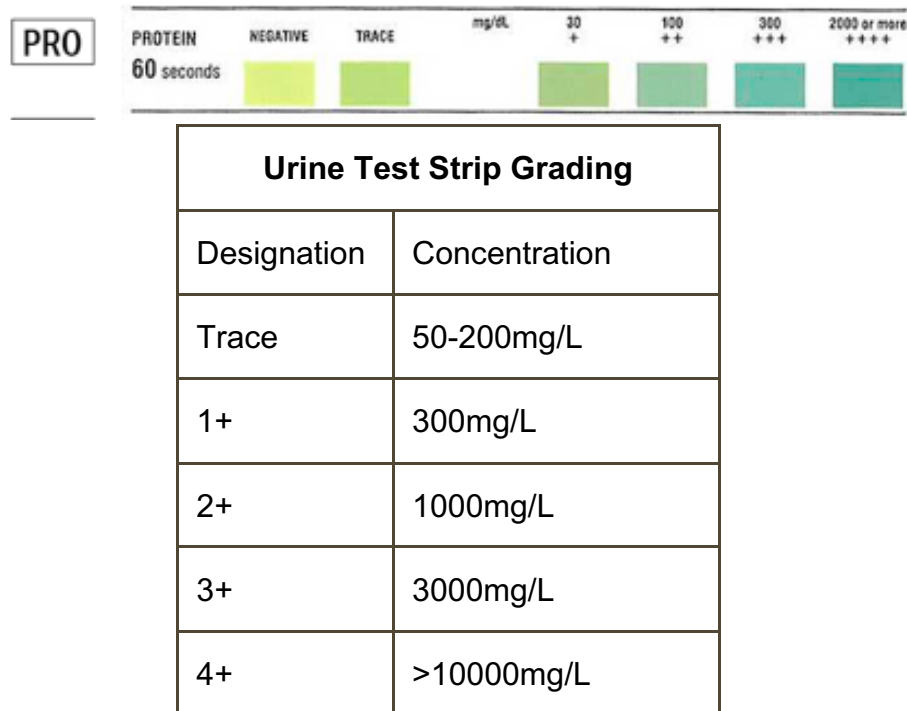


Figure 11. Strip urinalysis interpretation[41]

For the past 30 years, people have performed their measurements of urine albumin by this method, which is questioned the lack of specificity for albumin. However, this method for albumin with urine samples has been employed for a long time due to its simple, sensitive and inexpensive advantages[17]. The design of this strip is based on color discrimination and dip methodology. These design can be used in our study. Besides, its detection limit does not fully cover the micro-albuminuria and its performance exhibits high false result. Therefore, it has clinical value to develop high sensitive urine test strip.

## 2.2 Strip design based on drop methodology

### 2.2.1 Configuration of the lateral flow test strip

The Lateral flow test grows rapidly for diagnosis in clinical qualitative and quantitative analysis. It is usually performed over a test strip whose different plain porous components impregnated with immunoreagents are assembled on a plastic backing card[18]. The strip includes four important sections: sample pad, conjugate pad, nitrocellulose membrane and absorbent pad[19]. The reaction area of the nitrocellulose membrane is divided into test line and control line. It is an assay which is based on separation of components of a sample. The components' separation relies on difference in their movement via a sorbent. When fluid sample flows through different components of the strip, pre-immobilized reagents on the components become active[19].

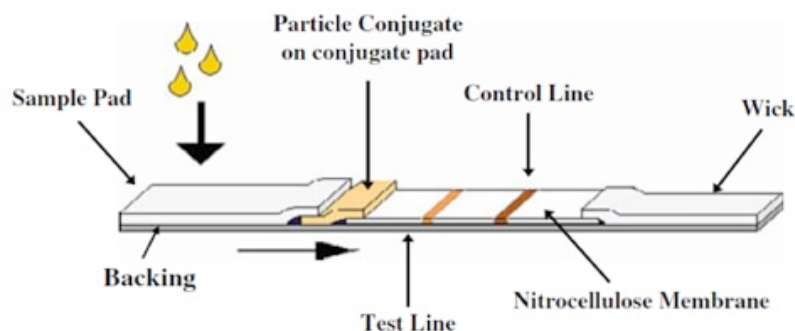


Figure 12. Typical layout of a lateral flow test strip[41].

The sample pad always uses cellulose or glass fiber. The fluid sample is dropped on this component to start assay. This pad enables transporting the sample to next component. Its material should have capability to transport sample smoothly, continuously and homogeneously. This pad also has function to pretreat the sample before it goes to next part, such as isolation of sample layers, removal of interferences, and adjustment of pH[19].

The conjugate pad is the place where labeled recognition bioprobe, such as antibodies or aptamers, is mounted. Glass fiber, cellulose and polyesters are usually applied to create conjugate pad. These materials are able to release labeled bioprobe

immediately when flowing fluid sample contacts with it. The labeled bioprobe should be stable because any variations such as dispensing or releasing of it may change results considerably[19].

The nitrocellulose membrane is the most critical component to determine strip's sensitivity. A good membrane should provide excellent binding to capture bioprobes. It should have high affinity for specific biomolecules and less non-specific adsorption in the test and control lines. Wicking rate of nitrocellulose membrane may affect assay sensitivity as well[19].

The adsorbent pad performs as a sink at the end of the strip. It supports to maintain sample's flow rate over the nitrocellulose membrane and to prevent backflow of the sample. Adsorbent capacity of holding sample may influence assay result[19].

Major steps to prepare a lateral flow strip include: production of antibody against target analyte, labeling recognition bioprobe, mounting reagents on components, and assembling components on the backing card[19]. Materials of components are not prepared specifically for albumin detection; hence they have difficulty to combine homogeneously. Same materials for sample pad, conjugate pad and membrane is helpful to achieve good sensitivity and reproducibility[19].

This assay has an advantage of combining recognition bioprobe and chromatography. It requires small sample volume without pretreatment and has better sensitivity and specificity than traditional colorimetric strip. Due to its low cost, it has high potential of commercialization. However, most applications of lateral flow test are qualitative or semi-quantitative because they are suffered from cross-reactivity and low biomolecules affinity with expected analytes[19].

### **2.2.2 Immunochromatographic assay (ICA)**

Immunochromatographic assay (ICA) is currently implemented by a lateral flow strip. Lateral flow ICA is applied to enhance sensitivity and specificity of the strip test. The design of this assay is a combination of chromatography and immunochemical reaction. Due to its rapid, simple and cost effective merits, immunochromatographic

strip is successfully used in medical diagnostics. Its market grows continuously at a rate of 6% per year[18].

Immunoassay includes the antigen reacting to the antibody, which leads to a physical isolation of the 'bound' antigen from the 'unbound' antigen in the heterogeneous immunoassay. On the other hand, homogeneous immunoassay asks for no physical separation. The antibody is used as a recognition bioprobe during ICA. The immunochemical interactions enable the process of binding to target analyte. It can be synthesized against specific target analytes. Mice are utilized to produce antibody which applies to detect analyte from human sample[19]. There are at least three different antibodies prepared. The antibodies need to have highest affinity. The priority is not equilibrium but the kinetic binding constant[18]. There are two methods to execute immunochromatography: sandwich ICA and competitive ICA.

#### **2.2.2.1 Methods: sandwich ICA and competitive ICA**

##### **Sandwich ICA**

For sandwich ICA, typical labels are enzymes, nanoparticles and fluorescent dyes, which are coated by antibody or aptamer and immobilized at conjugate pad. A primary antibody which aims to the target analyte is mounted on the test line. A secondary antibody which is against to the labeled antibody is mounted on the control line[19].

Sample with analyte is dropped onto the sample pad first and then flows to other components of the test strip. At conjugate pad, the immobilized labeled antibody grasps the target analyte and contributes to the formation of analyte-labeled antibody complex. Then the complex flows to nitrocellulose membrane under capillary action. At test line, the complex is grasped by the primary antibody. The analyte forms a sandwich structure which is between labeled antibody and primary antibody. At control line, the excess labeled antibody is captured by secondary antibody. At last, residual sample flows to absorption pad. Color intensity at test line is relevant to the concentration of target analyte. Appearance of color at control line guarantees there is enough labeled antibody to react with target analyte[19].

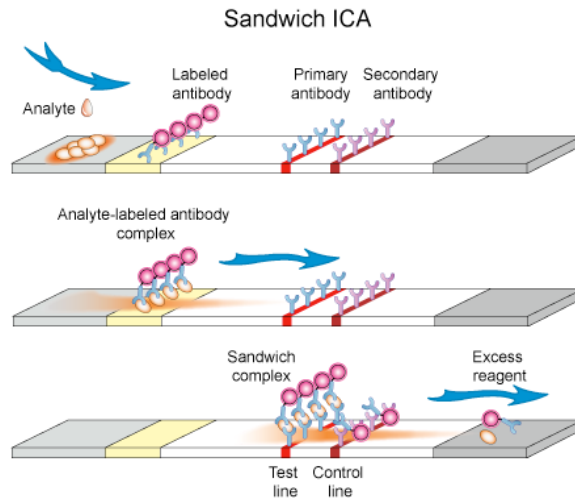


Figure 13. Sandwich ICA[41].

### Competitive ICA

Competitive ICA suits for low molecular weight compounds which are hard to bind two antibodies at the same time. In contrast to sandwich ICA, absence of color at the test line indicates the appearance of analyte. Presence of color at both test and control lines means negative result. After fluid is applied onto sample pad, it reacts to labeled antibody at the conjugate pad. Test line is immobilized by analyte conjugated primary antibody. Control line contains secondary antibody which captures labeled antibody. When fluid reaches the test line, analyte conjugated primary antibody will capture the labeled antibody if the target analyte is absent or presents at a low concentration, which means most sites of labeled antibody are vacant. The target analyte and the one which is conjugated primary antibody compete to capture the labeled antibody at the test line[19].

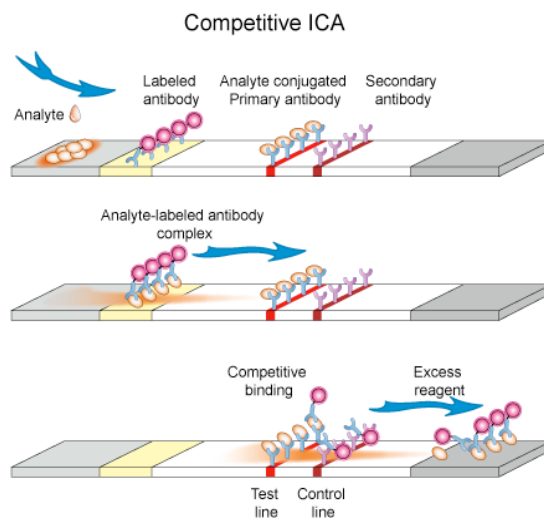


Figure 14. Competitive ICA[41].

### **2.2.2.2 Labels: colloidal gold nanoparticles and fluorophores**

Frequently used labels in ICA are colloidal gold nanoparticles, organic fluorophores and enzymes. The label should be detectable at very low concentration and sustain its properties after conjugating with antibody. This conjugation also should not change antibody's feature. A good label is easy to conjugate with antibody and has stability over a long period of time. The label which gives direct signal intensity is preferable[19].

#### **Colloidal gold nanoparticles**

Colloidal gold nanoparticles are the most often applied labels in ICA. Colloidal gold is inert and provides perfect spherical particles. The properties of these particles include high affinity with proteins and reveal excellent optical signal. Sensitivity is determined by molar absorption coefficient and amount of colloidal gold nanoparticles in target analyte[19]. Qualitative or semi-quantitative analysis can be performed via producing color by gold nanoparticles. However, its utility is limited when highly quantitative result is demanded[19]. Dazatiev's study shows that the composition's change of antibody-colloidal gold conjugate will vary the detection limit by two orders of magnitude[18]. Its analysis performance is also influenced by the method of reagent immobilization[18].

#### **Fluorophores**

Fluorophores are utilized as labels in ICA and the level of fluorescence is applied to quantitate the concentration of target analyte. Fluorescent microspheres represent much better sensitivity than gold colloidal. High brightness is required in this quantitative method. The inorganic quantum dots (QDs) are nanoscale semiconductor materials. Comparing with typical organic fluorophores, QDs provide more stable and sensitive results. A study states that QDs are 20 times brighter and 100 times more stable than conventional fluorophores[19]. The protein detection required high sensitivity is accomplished by employing QDs. However, under some conditions, some QDs display risks to human health and environment. Disadvantage of quenching is linked with QDs which contribute to reduce sensitivity[19].

## **2.2.3 Fluorescent immunochromatographic assay (FICA)**

A fluorescence immunoassay uses a fluorescent label accompanied with a fluorometer for detecting[20]. For quantification by the test strip, fluorescent spectrophotometer is used for measuring fluorescent intensity performed at test and control lines. Fluorescent brightness of test line is increased by an increasing concentration of target analyte in sandwich ICA, with a decrease in competitive ICA [19]. For the accurate quantitative test, the intensity of the bound label is relied by image processing of the fluorescence, instead of a simple visual test. The detectors provide result and eliminate subjective interpretation. Most tests require immunochromatographic strips combined with a portable detector.

### **2.2.3.1 Aggregation-caused quenching (ACQ) effect**

The studies currently focus on luminescence in solution state. The conclusion derived from solution investigation cannot be employed in the concentrated solutions. The reason is that many fluorophores, such as organic fluorophores and QDs, have very different light-emitting expression in dilute and concentrated solutions[11]. Conventional fluorophores emit light but are often quenched at high level solution or in an aggregation state. This phenomenon is named as aggregation-caused quenching (ACQ). The ACQ effect significantly restricts the labelling degree of fluorophores. The researchers have to apply dilute solutions of fluorescent bioprobe for acting as biosensor, which contributes to compromising sensitivity and difficulty of tracing biomolecules. The ACQ effect may also occur in the dilute solutions because the fluorophores incline to aggregate on the surface of biomolecules and cluster in the hydrophobic cavities of the folding structure, leading to quenching the emissions[10]. The cause for this process is mechanistically related with the 'formation of aggregates'[11]. Most of the ACQ fluorophores have planar structures. The aggregation generates  $\pi$ - $\pi$  stacking interactions and results in non-radiation species as excimers[11, 12]. This process leads to the observed ACQ effect. The application of dilute solutions results in many issues. The emissions from the solutions are very poor, which leads to weak sensitivity during applying fluorescence

to monitor quantities of biomolecules. The sensitivity is not able to be improved by employing high fluorophore level due to the ACQ effect[10].

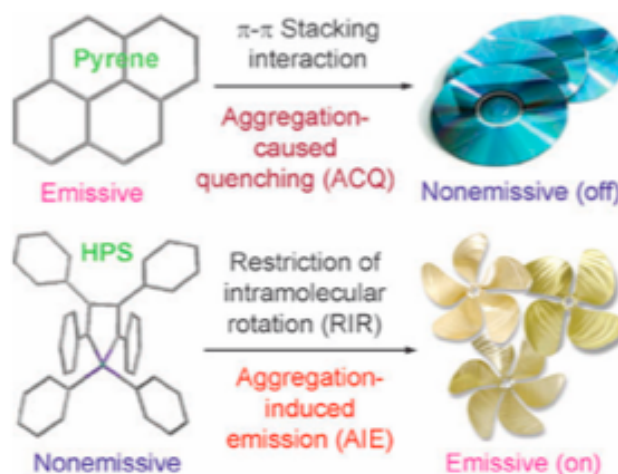


Figure 15. The comparison of ACQ and AIE effects [14]

### 2.2.3.2 Considerations for design improvement

It is necessary to optimize the performance of the strip. To innovate technologies for synthesizing reagents and creating inexpensive device to read test strips is important. Sensitivity of ICA strip is enhanced by changing physical parameters, including concentration of reagents on different component, label modification, and pre-incubation of sample with labeled antibody[19]. Improvement in materials may also help to enhance sensitivity, specificity and reproducibility of existing ICA method.

#### Raw material selection

The test strip should be stable during storage. The component of the reaction medium should be optimized to decrease non-specific adsorption. The carriers have different pore structure to support different liquid mobility. Dzantiev suggests that the use of fine-pore nitrocellulose membranes can improve specific interactions[18]. The complicated production process raises risks on reliability of assay.

#### New fluorescent label

Innovation is considered to focus on improving analytical procedures by employing new labels[18]. The label is detectable at very low concentration and is available for simple conjugation. For conventional fluorophore, the labeled antibody should preserve reactivity and detectable feature. It should have no specification with other components of the sample or with the chromatographic carries[18]. The traditional



fluorophores have no selectivity to analyte, therefore they need to label on the antibody which aims to analyte specifically. The new AIEgen can overcome this drawback due to its selectivity to analyte. It works like labeled antibody. High selectivity and sensitivity are criteria for AIEgen bioprobe to be utilized. The selectivity largely relies on the affinity of specific recognition components and receptors. The sensitivity relies on the brightness of the fluorescence and the comparison of the emissions before and after the binding reaction.

### **Reagent concentration**

The maximum permissible albumin concentration in urine is very low, so the test strip must detect at least 30mg/L. This asks for improving existing method to obtain test result with extreme detection limit. The strategies of decreasing the detection limit include: change the preparation procedure of the sample, increase the test signal, and change the impregnated reagents' concentration to control the kinetic conditions of reaction. The relationship between analyte's concentration and label's signal will support to provide final results. The reaction between reagent (antibody or AIEgen) and analyte is concentration dependent. The concentration of the reagent will affect the detectable number of the analyte at low concentration as well as the number of non-specific binding of the label[18]. Concentration of target analyte decides applicability of reagent as recognition bioprobe[19]. It is important to adjust the proportions of reagents to achieve a required minimum detection limit, especially for quantitative tests. There are high requirements for accuracy but it is hard to balance a low detection limit and high accuracy at the same time.

### **Reaction time**

The time of the interaction between the reactants in homogeneous and heterogeneous reaction is also an important factor. It must be long enough to complete the chemical reactions. The duration time can be balanced by choosing a suitable carrier and reaction medium.

## 2.3 AIEgen applications

There is a large amount of outstanding researches which have been done in the area of AIEgen development over the past year. These AIEgens are employed to high technical applications such as fluorescence sensors for explosive, pH, pressure, ion, temperature, viscosity, etc.; immunoassay markers; polarized light emitters; biological probes for protein, RNA, sugar, DNA, phospholipid, etc.; active layers in fabrication of organic light-emitting diodes; the poly (acrylamide) gel electrophoresis (PAGE) visualization agents; monitors for layer-by-layer assembly; multi-stimuli responsive nanomaterials; reporters for micelle formation[10].

In this section, we illustrate some recent progress in the AIEgen technological applications. Hong's team reports that AIEgens have already been designed with emission color covering the whole range of visible lights in order to obtain full-color display. Hence, many OLEDs applying the AIEgen as the emitting layers are fabricated for electroluminescence devices[11]. The AIEgen also can be used as useful analytical tools, such as selective and sensitive chemosensors and bioprobes, to monitor and quantify the environmental pollutants ( $\text{Hg}^{2+}$ ,  $\text{Zn}^{2+}$ ,  $\text{Ag}^+$ ,  $\text{CN}^-$ )[21]. Some AIEgen sensors have been designed for small molecules detection, such as glucose, nerve agents, and  $\text{CO}_2$ . The sensing of  $\text{CO}_2$  which has huge influence on the global climate is one of the significant societal implications. Hong's team uses an amine solvent to dissolve Hexaphenylsilole (HPS), one type of AIEgen, for quantitative detection of  $\text{CO}_2$  gas[11]. Xie's team designs an AIEgen based test strip for detecting gaseous phosgene which is an industrial chemical intermediate and highly toxic gas. The team fabricates OPD-TPE-Py-2CN for sensitive detection and the detection limit of 1.87ppm is much lower than harmless concentration limits[9]. In recent decades, the research of carbohydrate-protein interaction becomes popular due to its involvement in many biological processes such as inflammation. The development of AIEgen for studying protein conformation supports these investigations[22]. The AIEgen is not only used as fluorescence sensor, but also can be used for cell imaging. For example, the fluorescent silica nanoparticles (FSNPs) with AIEgen feature has no

toxicity to living cells and is employed to selectively stain the cytoplasm of HeLa cells[11].

The AIEgens as smart materials have the ability to change the emission properties according to different stimuli, such as vapor fuming, mechanical force, thermal heating, and photon irradiation. Chi's research constructs an asymmetric molecule SFPC which can integrate the features of AIE, mechanoluminescence, and delayed fluorescence into one compound. This impressive material can be used as mechanical sensor to sense pressing or grinding[21]. Li's study develops another AIEgen named DPP-BO with fluorescence and phosphorescence dual emission under mechanical situation. The study proves the effectiveness of it as a mechanical stimuli responsive sensor[21]. To sensitively monitor pathogenic bacteria, such as drug resistant bacteria, is important in food safety inspection. Gao reports several AIEgens for luminescent image of bacteria. One of them is AIE-2Van which can recognize Gram-positive bacteria[21]. Qiu's research presents a simple and sensitive method for measuring glass transition temperature by applying AIEgen TPA-BMO. The detection captures fluorescent images of polymer films, which are doped with AIEgen, under different temperature. The images are calculated by a MATLAB program to evaluate the fluorescent light intensity. Then the correlation of temperature and light intensity can be obtained. The measurement shows sensitivity and reliability [23].

In conclusion, the AIEgens in various applications perform well and they are expected to serve as practical platforms for more wide ranging applications.

## **2.4 AIEgens for health monitoring**

The disease biomarkers require accurate and sensitive detection methods. The AIEgens can be developed to diagnose various disease. We review some notable AIEgens for disease detection. Tang's team designs an AIEgen bioprobe IDATPE to quantify the creatinine. The human serum albumin concentration can be measured by another AIEgen BSPOTPE[21]. IDATPE and BSPOTPE can combine together for early detection of kidney disease. Yang's research develops an AIE-active

metallacycle to detect heparin, which is a widely applied anticoagulant. Heparin concentration can be determined of 0-28 $\mu$ M by this AIEgen bioprobe with high selectivity. Tang also designs an AIEgen HPQ-TBP-I to interact with heparin and quantitate its concentration with the detection limit of 22nM[21]. In Parkinson's disease, the  $\alpha$ -synuclein with abnormal aggregation and fibrillation plays an important role. Tang produces an AIEgen named TPE-TPP to enable monitoring fibrillation process with a high sensitivity. The TPE-TPP can be utilized for early detection of Parkinson's disease. An AIEgen bioprobe composed of a TPE and a peptide component is employed to bind specifically with amyloid fibrils. Ghorai and Jana states that this property can be applied to detect Alzheimer's disease due to 4-fold stronger sensitive signal comparing with traditional probe[21]. The pathogenic bacteria detection is crucial in clinical infection diagnosis. Zhang designs a multi-fluorescence array for eight kinds of bacteria detection. This array is composed of five TPE-derived molecules to identify normal bacteria and multidrug-resistant bacteria for infected patients[21]. Jiang designs a TPEPyE with AIE feature for detection of urinary tract infections. This AIEgen bioprobe monitors bacterial lipopolysaccharide in urine sample through fluorescent turn-on feature and the sensitivity of detection can down to nanomolar[24]. Apart from these, the various AIEgen are developed for diagnosing diseases, such as prostate cancer etc.

The AIEgens for health monitoring develop fast. However, these AIEgens are still in the laboratory stage and lack of commercial applications in real world, such as AIEgen based urine test strip. Therefore, it is necessary to apply these bioprobes for disease diagnosis and furthermore to design portable diagnostic platforms.

## **2.5 Current research of BSPOTPE for urine albumin detection**

### **2.5.1 BSPOTPE characteristics**

The AIE bioprobe of BSPOTPE for quantitating HSA is combined to diagnose the related kidney diseases[21]. Hong's team has finished several tests to find out the

characteristics of BSPOTPE for quantitating albumin in solution[4]. The research of Forster Resonance Energy Transfer (FRET) states that BSPOTPE has the ability to access to HSA. The study also shows the possible location of BSPOTPE in the hydrophobic cavity in the HSA folding structure[4]. BSPOTPE's fluorescent quantum yield is 0.37% in water and 17.5% in acetonitrile because BSPOTPE is insoluble in organic solvents and its luminogen molecules aggregate in acetonitrile[4]. The BSPOTPE in PBS is weakly luminescent without HSA. After an amount of HSA is dropped into BSPOTPE solution, the solution is luminescent. The non-luminescent BSPOTPE enables emitting under HSA appearance. The fluorescent intensity increases by raising the concentration of HSA.

Hong's research also examines the feasibility of HSA quantitation in artificial urine. According to the results, the sensitivity of BSPOTPE detecting HSA is not influenced by the miscellaneous bioelectrolytes and urea. Because of the AIE property of BSPOTPE, the detection limit is able to be altered by changing the concentration of fluorogen[4]. The result presents that the rate of the fluorescent raise is fast at low concentrations of HSA but becomes constant at HSA concentration  $> 1\mu\text{M}$ . Figure 16 shows that the fluorescent intensity raises around 300-fold at HSA concentration of  $10\mu\text{M}$ [4]. The BSPOTPE presents a linear calibration curve at  $[\text{HSA}]=0-100\text{nM}$ , which makes the HSA quantitation possible over a broad concentration range[4].

The research also presents BSPOTPE as having good selectivity to albumin, for instance HSA and bovine serum albumin (BSA). A series of proteins and DNAs are chosen to test its selectivity. Figure 17 shows that none of these proteins have the capability to light up the BSPOTPE. The selectivity of BSPOTPE toward HSA keeps constant in artificial urine. This fluorescent bioprobe has a low detection limit which is down to  $1\text{nM}$  and a high selectivity toward albumin[4].

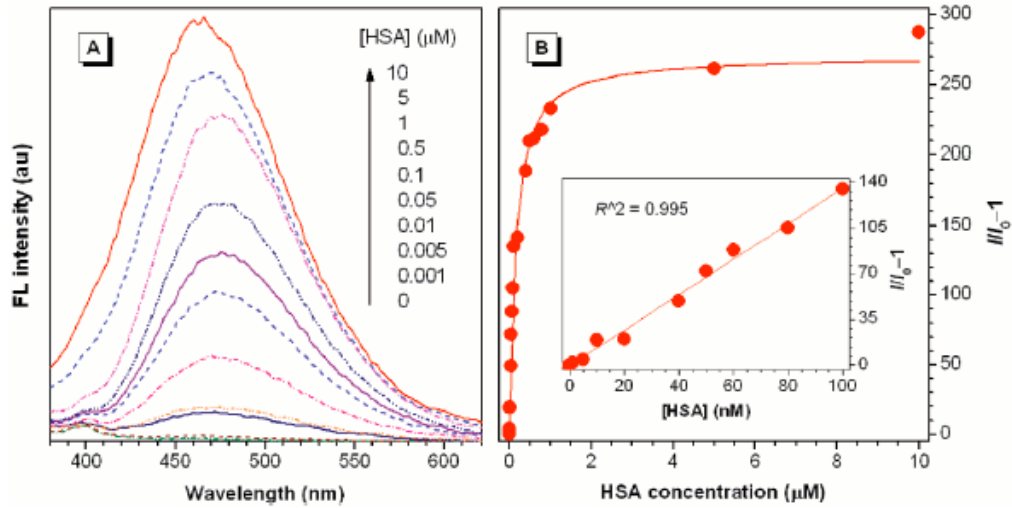


Figure 16. (A) FL spectra of BSPOTPE with different concentrations of HSA. (B) The change of FL intensity by different concentrations of HSA[4].

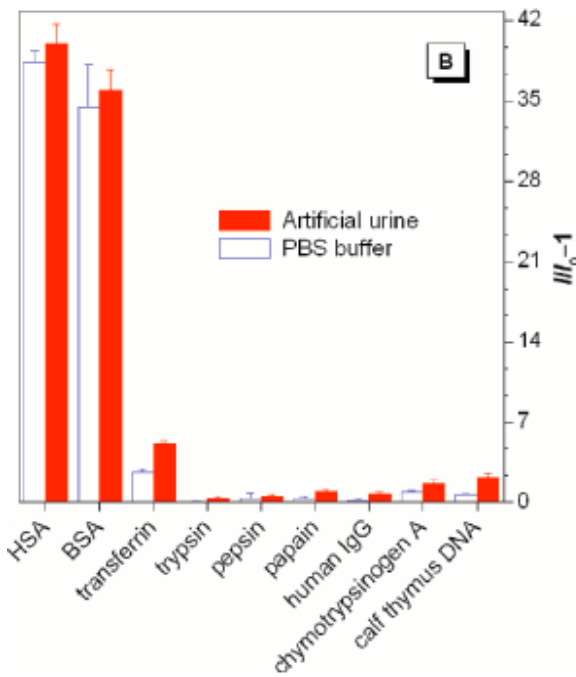


Figure 17. The intensity of BSPOTPE on different proteins in artificial urine and PBS [4].

Chen's study applies AIE-active probes BSPOTPE and IDATPE for detecting and quantitating of albumin and creatinine, respectively[21]. IDATPE, another bioprobe with AIEgen feature, is applied with BSPOTPE to evaluate mutual interference when both bioprobes are employed together for creatinine and HSA detection. A good correlation between fluorescent light intensity and creatinine concentration (0-100 μM) in artificial urine is obtained. This result enables to further development of BSPOTPE's clinical application[21].

## 2.5.2 Smartphone-based urinalysis using BSPOTPE bioprobe

Smartphone app-based monitoring tool for analyte detection has been gradually developed in recent years. Fang's team reports using a smartphone camera to detect PFOA and PFOS in a tap or groundwater by reading the color (RGB: Red, Green, and Blue) of reaction results. The value of RGB is connected to the concentration with a LOD of 10ppb and a standard deviation of <10%[28]. Hou's team describes a smartphone-based dual-modality imaging system for quantitative detection of FICA strips. This imaging system is combined with an optical device designed with white and UV light for different strip detection such as fluorescent strips. The software uses Sobel operator algorithm to enhance the recognition ability of the test area. The results show that this system can provide various diagnoses based on strip analysis. The smartphone diagnosis becomes a potential technology for the next generation point-of care test in the near future[29].

The BSPOTPE bioprobe can be monitored by smartphone using image processing analysis as well. In Shaymaa's study, a new type of urinalysis device named uTester is developed to conduct reliable and portable quantitative detection of albumin in urine by applying the smartphone[13]. The device comprises an imaging housing which is a black box and can be attached to the smartphone with various dimensions and camera positions. The uTester employs BSPOTPE as a bioprobe and uses one test cuvette filled with this AIEgen reagent solution. The study measures fluorescent light intensity through taking the image of the emission light from the test cuvette by applying the smartphone. Afterwards processing and analyzing the image by software, at last presenting the light intensity values according to the image's luminance property which determines the amount of light emission[13]. The result shows that a prediction model of albumin concentration with linear correlation is obtained. Figure 19 displays this model with:  $x=(y-a)/b$ , where y is the image intensity value, x is the albumin concentration, a and b are the coefficients with 95% confidence interval obtained from the training data[13].

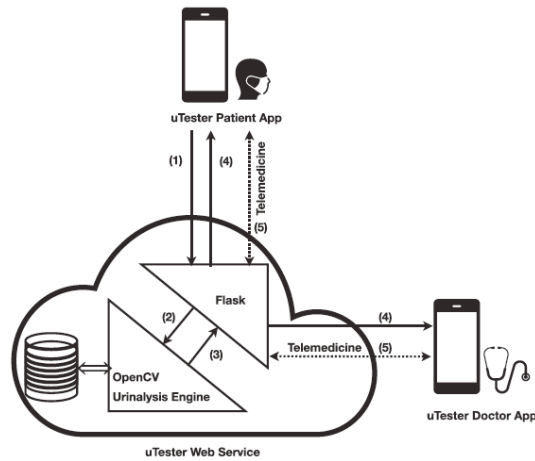


Figure 18. The workflow of uTester smartphone application for urinalysis[13].

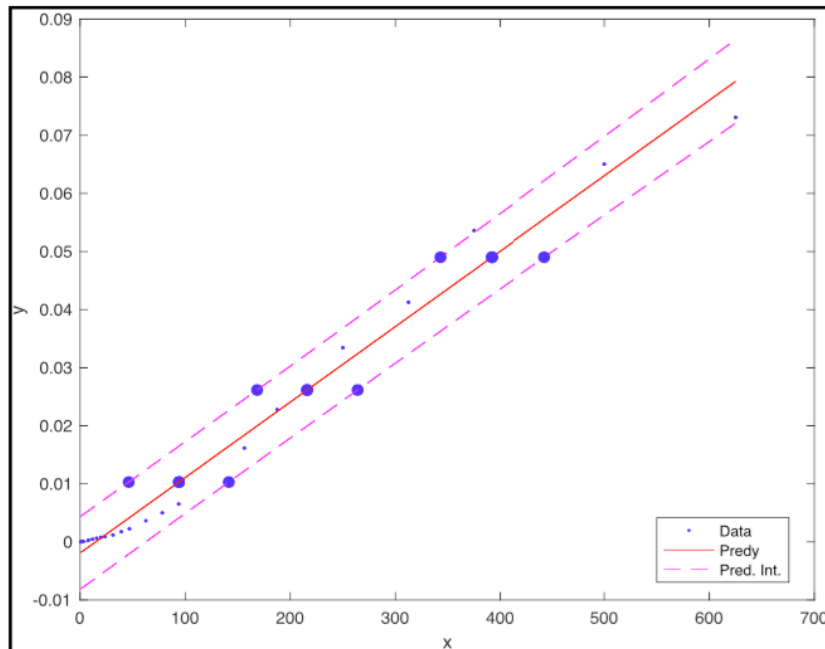


Figure 19. The linear prediction model with internals[13].

This device has the requirement of image quality such as intensity of color because a slight drift may result in inaccurate quantification. The human visual system senses colors by brightness attributes. In contrast, the computer describes colors by applying the RGB model. The RGB model is not the most appropriate means to exhibit images in the real world. Therefore, Shaymaa’s research chooses the HSL (Hue, Saturation, Lightness) model to transform the visible electromagnetic spectrum (color) into a digital signal because it is cognitive and intuitive for humans [13]. After the images are captured by the smartphone, the image software transforms the RGB color space into



the HSL color space and calculates the average values of the intensity band of the HSL color space from the cuvette selected area. Afterwards, it retrieves the average brightness value from the HSL color space to represent the luminance color band of the region [13].

Shaymaa's study provides a solution of smartphone clinical detection and proves that the uTester application has the ability to perform urinalysis and telemedicine by using BSPOTPE bioprobe. The evaluation of uTester has demonstrated the effectiveness of the device agnosticism as well as the feasibility of a smartphone-based device for quantitative urinalysis under liquid state[13].

In conclusion, the BSPOTPE works well in the artificial urine and is promised to apply to real urinary albumin detection[4]. It is necessary to design a simple bioassay test strip for clinical diagnostics by using this new bioprobe.

# Chapter 3: Materials and methods

## 3.1 Materials

### 3.1.1 Chemicals

All of the chemical reagents applied in this experiment, such as HSA, were purchased from Sigma-Aldrich unless otherwise stated. BSPOTPE was synthesized according to previously published procedures[4, 22]. Lab water was purified by a Millipore filtration system. All the experiments were implemented under room temperature unless otherwise noted.

### 3.1.2 Chemical sample preparation

The BSPOTPE solution, with a concentration of 50 $\mu$ M, was prepared by dissolving into an appropriate amount of deionized water. The solution of HSA was prepared by using artificial urine to a concentration of 3 $\mu$ M. Artificial urine was prepared by dissolving amounts of components in deionized water as following Table 1. The pH of the solution was 6.53, which was measured by a digital pH meter (Hanna pH meter, mode: HI 208-02).

All the solutions were stored at 4°C in the dark environment before use. Working solutions were prepared daily by appropriate dilution of the stock solution with either artificial urine or deionized water.

Chemicals	Molecular Formula	Molecular Weight (g/mol)	Concentration(m M)
Urea	NH <sub>2</sub> CONH <sub>2</sub>	60.06	200.00
Uric acid	C <sub>5</sub> H <sub>4</sub> N <sub>4</sub> O <sub>3</sub>	168.11	1.00
Creatinine	C <sub>4</sub> H <sub>7</sub> N <sub>3</sub> O	113.12	4.00
Sodium citrate dehydrate	HOC(COONa)(CH <sub>2</sub> COONa) <sub>2</sub> · 2H <sub>2</sub> O	294.10	5.00
Sodium chloride	NaCl	58.44	54.00
Potassium chloride	KCl	74.55	30.00
Ammonium chloride	NH <sub>4</sub> Cl	53.49	15.00
Calcium chloride	CaCl <sub>2</sub>	110.98	3.00

Magnesium sulfate heptahydrate	MgSO <sub>4</sub> 7H <sub>2</sub> O	246.47	2.00
Sodium bicarbonate	NaHCO <sub>3</sub>	84.01	2.00
Sodium oxalate	Na <sub>2</sub> C <sub>2</sub> O <sub>4</sub>	134	0.10
Sodium sulfate	Na <sub>2</sub> SO <sub>4</sub>	142.04	9.00
Sodium phosphate monobasic monohydrate	NaH <sub>2</sub> PO <sub>4</sub> H <sub>2</sub> O	137.99	3.60
Sodium phosphate dibasic anhydrous	Na <sub>2</sub> HPO <sub>4</sub>	141.96	0.40

Table 1. Component of artificial urine applied in this study[8, 25]

### 3.1.3 Test strip materials

The assay strip consisted of conjugate pad, nitrocellulose (NC) membrane, absorbent paper and self-adhesive plastic backing. All of these strip materials were purchased from Shanghai Jieyi Biotechnology Co., Ltd. These include materials for traditional scale reporting of pH, relative density, leukocyte esterase, hemoglobin/myoglobin, nitrite, protein, creatinine, glucose, ketones, urobilinogen and bilirubin[14]. The glass fiber as conjugate pad included two types: Fusion4 and Ahlstrom8964. The NC membrane included two types: Sartorius CN140 and Sartorius CN95.

The study included microstructure examination of individual raw material such as glass fiber and NC membrane. All types of material were tested by FEI Inspect F50 scanning electron microscope (SEM) platform. SEM produced image contained information of sample's surface topography and composition.



Figure 20. FEI Inspect F50 scanning electron microscope platform

### 3.1.4 Test strip configuration

Test strips were prepared in the laboratory to fit into a desirable configuration. The BSPOTPE was dispensed onto the conjugate pad. The NC membrane and absorbent paper were employed without treatment. Strips were prepared by a manual assembly. The components were cut into 10mm length and 10mm width individually. For the dip strip, only the conjugate pad was adhered to the plastic backing. For the drop strip, all three parts were laminated sequentially onto the adhesive backing and each part overlapped 1mm. Then the prepared strips were stored at 4°C inside a sealed plastic bag with desiccant for future use.

### 3.1.5 Other information

The fluorescent light intensity under the solution state was recorded on a Cary Eclipse Fluorescence Spectrophotometer. Fluorescent spectra of solution were measured in the wavelength range of 400-600nm using 365nm as the unique excitation wavelength.

Fluorescent light image of the strip was captured by a smartphone (Samsung Galaxy Note3) under a UV lamp with 365nm as an excitation source. The smartphone camera was set to close functions of flash and High Dynamic Range (HDR), because the HDR was employed to enhance the span between shadows and highlights in an

image. The ISO function controlled the camera sensor's sensitivity. It was set to 800 to optimize the image under low light conditions. The Auto White Balance (AWB) algorithms explained variations regarding to in visual sensitivity under changing ambient illuminant conditions. It was set to Daylight for preserving the color response as a constant. The camera captured images under Autofocus model[13].



Figure 21. Cary Eclipse Fluorescence Spectrophotometer

## 3.2 Methods

### 3.2.1 Assay procedure

The process of detecting HSA sample by test strip based BSPOTPE included four steps: experiment set up, test strip preparation, image capture and image evaluation.

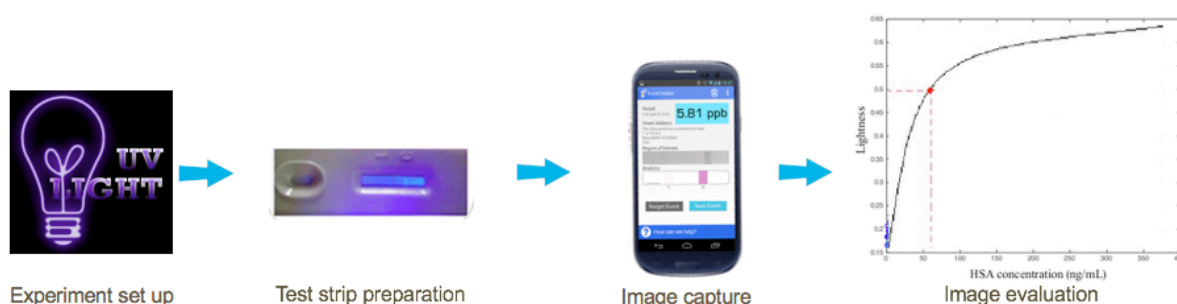


Figure 22. Process of the experiment

The experiment was performed in a dark room. The UV lamp was located at 15cm from the strip sample. Under this exciting UV light of 365nm, the prepared strip emitted fluorescent light. After assembling the test strip by different components, the HSA solutions with different concentration were added onto the strips. The prepared strips had features of corresponding fluorescent light intensity, which were determinant of HSA concentration. The smartphone was at 25cm from the strip

sample and captured the strip image under the UV light. A series of signal rich images were obtained. These images carried information of light intensity and could represent the HSA concentrations.

All strip images were processed by existed MATLAB code to analyze the brightness grade. The code was proved effectively by the research of Shaymaa Akraa and Ravichandran Rasiyah[13]. The Appendix 2 exhibited the MATLAB code applied. The values of fluorescent light intensity were calculated and displayed. Ultimately, the correlation between image intensity and HSA concentration in urine sample could be carried out.

### **3.2.2 Test strip design methodology**

#### **3.2.2.1 Method selection**

The design of test strip was based on rapid analysis with a minimum number of steps, therefore our design preferred simplified strip. First, we tried to use a cross flow pad to detect the fluorescent light intensity. This method only applied one kind of material glass fiber rather than four. The cross flow pad was the place dispensing reagent and interacting with the sample. After dropping sample onto the pad, the result showed no homogeneity which might lead to an inaccuracy image processing. The reason might be that the drops were concentrated in the center of the pad and the fluid was hard to push fluorogen to each area homogeneously.

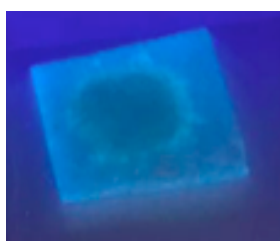


Figure 23. The absence of homogeneity after dropping the sample on cross flow pad

The aim of designing a new strip was to obtain a homogeneous image with rich signal information after the analytical reaction. To improve the homogeneity of images, we developed two methods: dip and drop methods. Dip method kept the same glass fiber pad but changed the means of dropping the sample on the pad, substituted by dipping the pad into the sample. Consequently, each area of the pad

could have reaction uniformly. This method required glass fiber having the features of uniform absorption, prominent wet-strength and handling, no hard spot or density changes, and no airborne fibers[26]. Drop method didn't change the means of sample dropping but added one more homogenous material as the result showing area. This method combined glass fiber with NC membrane, followed by absorbent paper. We captured images on the NC membrane whose microstructure supported a uniform and high-resolution image.

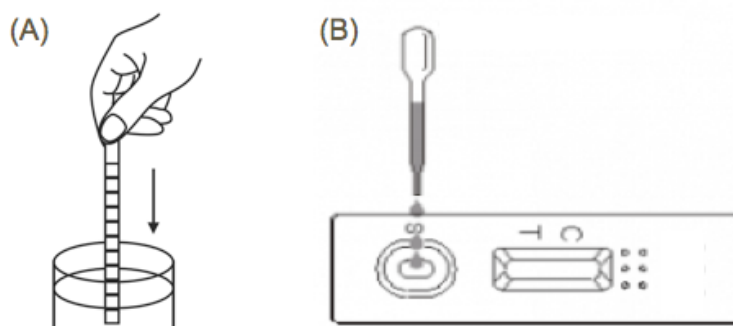


Figure 24. Method selection (A) dip method[42] (B) drop method[43]

### 3.2.2.2 Dip and drop methods

In this study, the designs of test strip are based on two methods: dip and drop. The strip based on dip method is immersed completely into urine sample in several seconds. Then extracting it and waiting to detect. It only contains one pad which is coated with reagent and is also the reaction zone. The pad material and its holding capability of the reagent are the key indexes for strip design.

The drop method is also known as lateral flow assay which dropping urine sample onto the assembled strip. The original strip is composed of four parts. The fluid flow through each part sequentially. This approach allows the removal of unreacted compounds from the reaction part and uses the reaction part to concentrate and to monitor the target complex[18]. The material selection of each part as well as configuration design are paramount for the final result.

It is crucial to optimize both strips' performance. In the following chapters, we consider different approaches to enhance analytical results by applying different strip materials, reagent concentration and incubation time.

# Chapter 4: Results and discussion

## 4.1 Strip based on dip method

### 4.1.1 Strip design

The strip based on dip method was composed of only one pad whose dimension was 10mm×10mm. The pad was made of glass fiber due to its robust absorption ability of reagent and rich signal information of the picture. The glass fiber pad was coated by BSPOTPE with certain concentration. The coated pad performed as conjugate pad as well as reaction area. It enabled urine sample meeting BSPOTPE uniformly and exhibiting the result directly. After mounting BSPOTPE onto the glass fiber, the dry pad was assembled to a plastic backing. The procedure of the test included immersing the pad area of the strip into the urine sample for several seconds, then extracting it from the sample and waiting for a while to support reaction time. At last, the strip was examined by taking a picture of the reaction pad. The intensity of the reaction fluorescence of the test pad was monitored by measuring the amount of light emitted from the surface of the test pad. The light intensity value of the pad could be calculated by using a specific algorithm. This strip design could make the sample contact with reagent homogeneously because each part of the strip pad was dipped into sample synchronously. Consequently, the homogeneity of the image brightness could be optimized by this methodology.

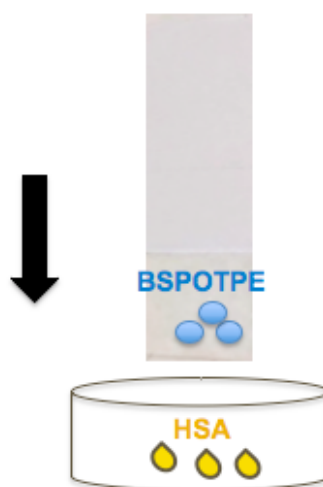


Figure 25. Strip based on dip method



### 4.1.2 Glass fiber

The conjugate pad was the place where BSPOTPE was dispensed. A material of conjugate pad should immediately release BSPOTPE when it contacted with moving liquid sample. It also should have excellent hydrophilicity. Glass fiber was employed to make the conjugate pad for both dip and drop methods. Nature of the glass fiber had an effect on the capability of store and release BSPOTPE. Poor selection of the glass fiber might adversely influence the sensitivity of an assay.

Here were two types of glass fiber: Fusion4 and Ahlstrom8964. Both glass fibers were manufactured from high purity and 100% FDA compliant alpha cotton cellulose with no additives which might cause accumulated backgrounds or other interference in a detection system. Because of their intrinsic properties, glass fibers had application in chromatography techniques where solute loading volume was not heavy[26]. Their features and properties were checked in order to better selection.

Under the same dimension, Fusion4 had the relatively thinner feature than Ahlstrom8964 but heavier weight. The appearance of both was the brilliant white color which could reflect more than 96% of visible light[27]. The surface of Fusion4 was uniform comparing to Ahlstrom8964, which could provide good resolution. Ahlstrom8964 was rugged on the surface and each fiber was clearly identified by eyes.

<b>Glass fiber name</b>	<b>Size(mm×mm)</b>	<b>Weight(g/m<sup>2</sup>±10)</b>	<b>Thickness(mm±0.05)</b>
<b>Fusion4</b>	210×300	76.9	0.38
<b>Ahlstrom8964</b>	210×300	75.5	0.42

Table 2. Glass fiber specification[44].

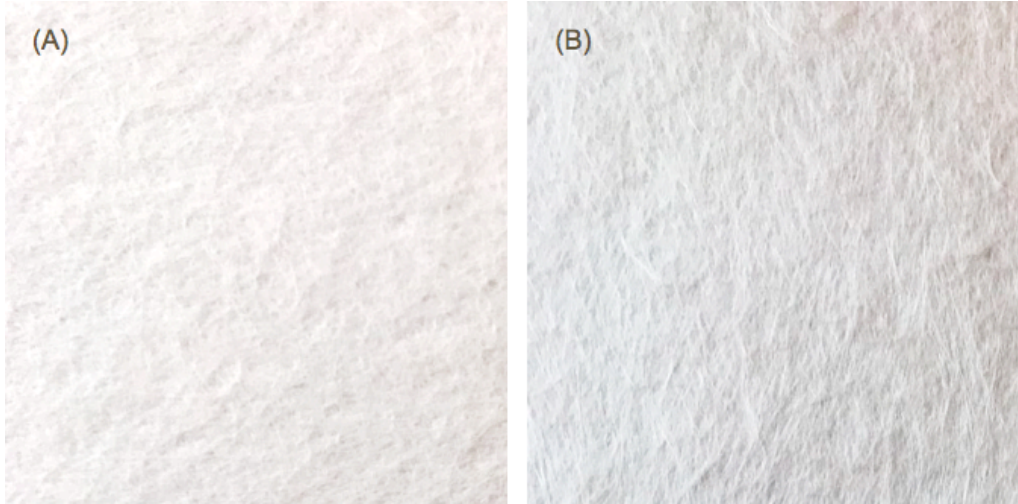


Figure 26. The appearance of original glass fiber under the visual light.

(A) Fusion4 (B) Ahlstrom8964

The structure of both glass fibers was examined under the SEM. The result showed that Fusion4 had thinner fibers and a large amount of binder among fibers. Hence, it owned high density of fibers. The Ahlstrom8964 was a binder-free microfiber glass. There were many cavities across fibers and the dimension of each cavity was large. Currently, to increase its stability, the glass fiber was cross-linked with glutaraldehyde or organic bi-functional silanes such as Fusion4[27]. This property enabled fibers to condense and resulted in high levels of resolution.

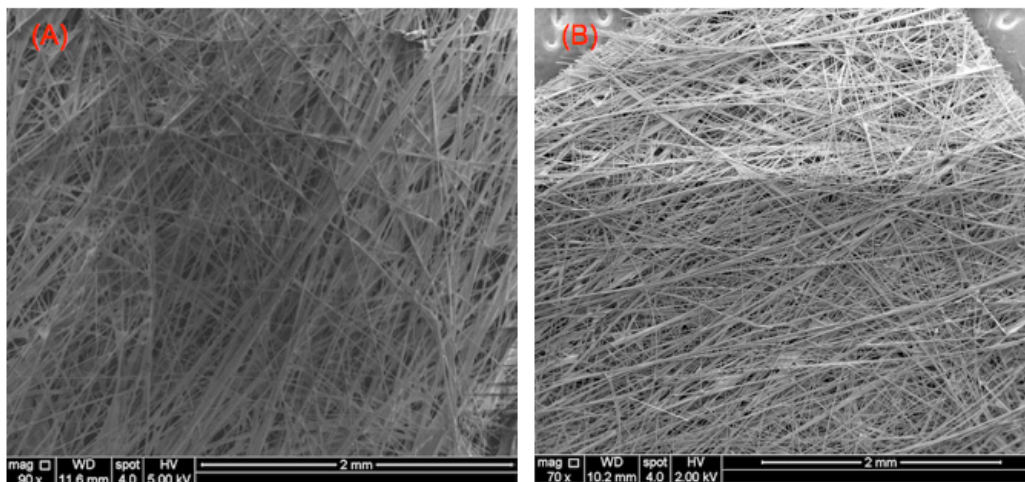


Figure 27. The appearance of original glass fiber under the SEM. (SEM @90/70X; bar=2mm).

(A) Fusion4 (B) Ahlstrom8964

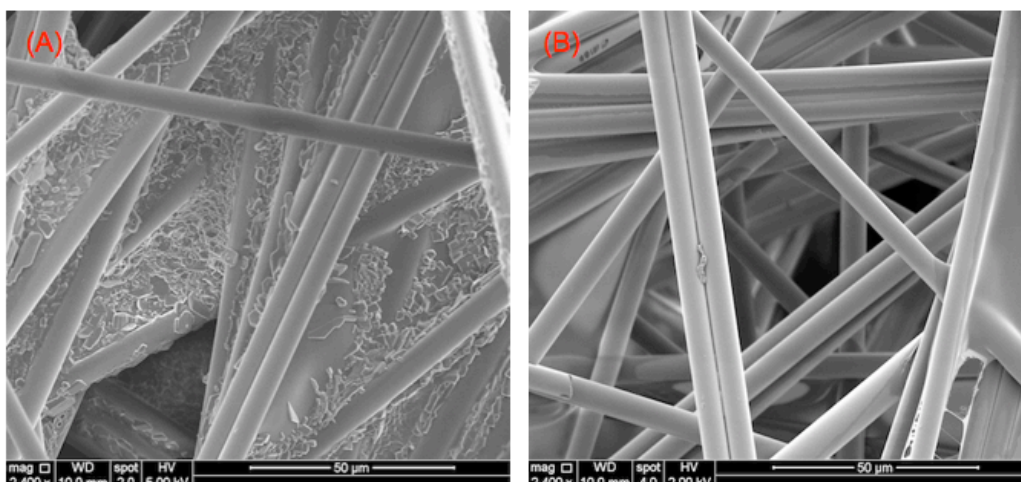


Figure 28. The appearance of original glass fiber under the SEM. (SEM @2400X; bar=50 $\mu$ m).

(A) Fusion4 (B) Ahlstrom8964

After coating BSPOTPE concentration of 50 $\mu$ M with 50 $\mu$ L, two glass fibers with a size of 10mm $\times$ 10mm were checked under the 365nm UV light and the SEM. Both glass fibers became luminescent under UV spectrum. The Fusion4 was much brighter than Ahlstrom8964, which meant it could hold more amounts of BSPOTPE within fibers. Brighter image provided much richer signal for processing and analyzing. The SEM Figure 30 illustrated that the BSPOTPE was immobilized onto the surface of fibers. Due to the high density, Fusion4 had much larger surface area of fibers and could carry more BSPOTPE.

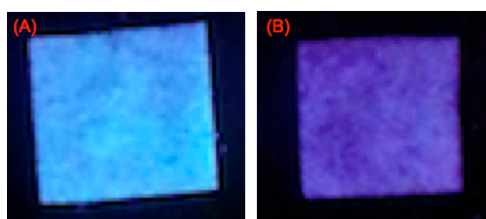


Figure 29. Glass fiber (10mm $\times$ 10mm) coated with BSPOTPE(50 $\mu$ M, 50 $\mu$ L) under 365nm UV light.

(A) Fusion4 (B) Ahlstrom8964

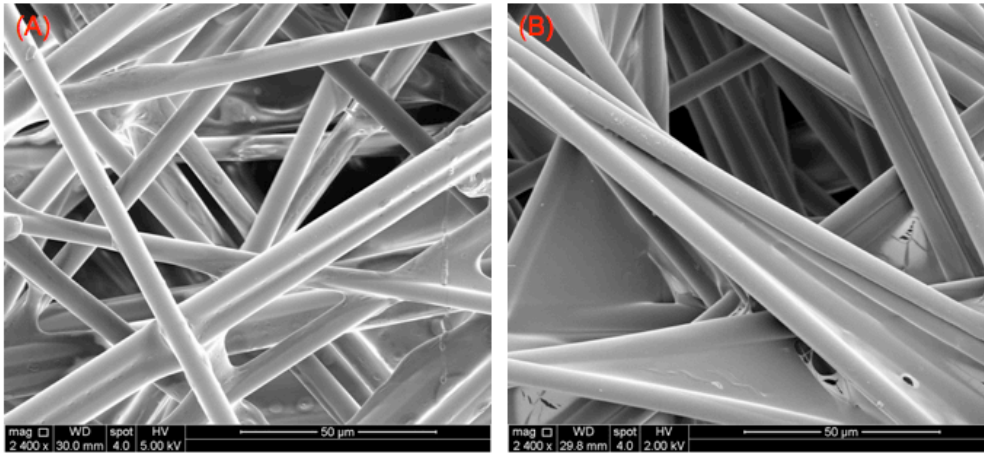


Figure 30. Glass fiber (10mm×10mm) coated with BSPOTPE(50μM, 50μL) (SEM @2400X; bar=50μm)

(A) Fusion4 (B) Ahlstrom8964

To compare these two glass fibers, Fusion4 had largely adsorbing BSPOTPE due to the higher density of fibers. Its final image could achieve enough brightness threshold to distinguish the difference with each sample, which represented abundant signals could be obtained. In addition, it offered uniform surface which lead to high resolution when the image was captured. Conversely, Ahlstrom8964 had drawbacks on both brightness and resolution. As a result, Fusion4 was chosen as conjugate pad due to its better sensitivity for assay.

#### 4.1.3 Reagent concentration optimization

Apart from optimizing the strip individual material, we also had to determine the concentration of BSPOTPE which performed as the reagent in the strip test. When BSPOTPE encountered with HSA, the binding reaction would occur immediately because of its high selectivity toward HSA. After binding, the fluorogens as bioprobes labeled HSA. The intensity of fluorescent light could be applied to quantitate the concentration of HSA in a urine sample. Appropriate BSPOTPE concentration decided the amount of fluorogens mounting onto the glass fiber.

The experiment used the different concentrations of BSPOTPE solution to have a reaction with urine samples with a range of HSA concentrations. We chose BSPOTPE concentrations of 5μM, 10μM, 20μM, 30μM, 50μM by 300μL to mingle with 2700μL of artificial urine with an increasing HSA concentration. After a 10-minute

incubation time, the performance of the reaction was examined by fluorescence spectrophotometer under the 365 nm excitation wavelength of UV spectra. The fluorescent light spectra were recorded in the wavelength range of 400-600nm.

The result showed that BSPOTPE solution was feebly luminescent at 365nm in the absence of HSA. When the HSA was added, the BSPOTPE solution became luminescent. The fluorescent light intensity kept rising with an increase in the HSA concentration. The high concentration of BSPOTPE solution had a large magnitude of fluorescent light intensity value. The enhancement rates of fluorescent light intensity were fast at lower HSA concentration and became almost constant at higher HSA concentration. The high BSPOTPE concentration presented a higher slope at lower HSA concentration and entered into a stable stage at larger HSA level, which meant it could achieve better sensitivity to quantitate lower HSA concentration and detect a broader range of HSA concentration with a precise result. The BSPOTPE concentration with 50 $\mu$ M was applied to design the strip in this study because it provided a larger detective range at [HSA]<2 $\mu$ M with higher sensitivity.

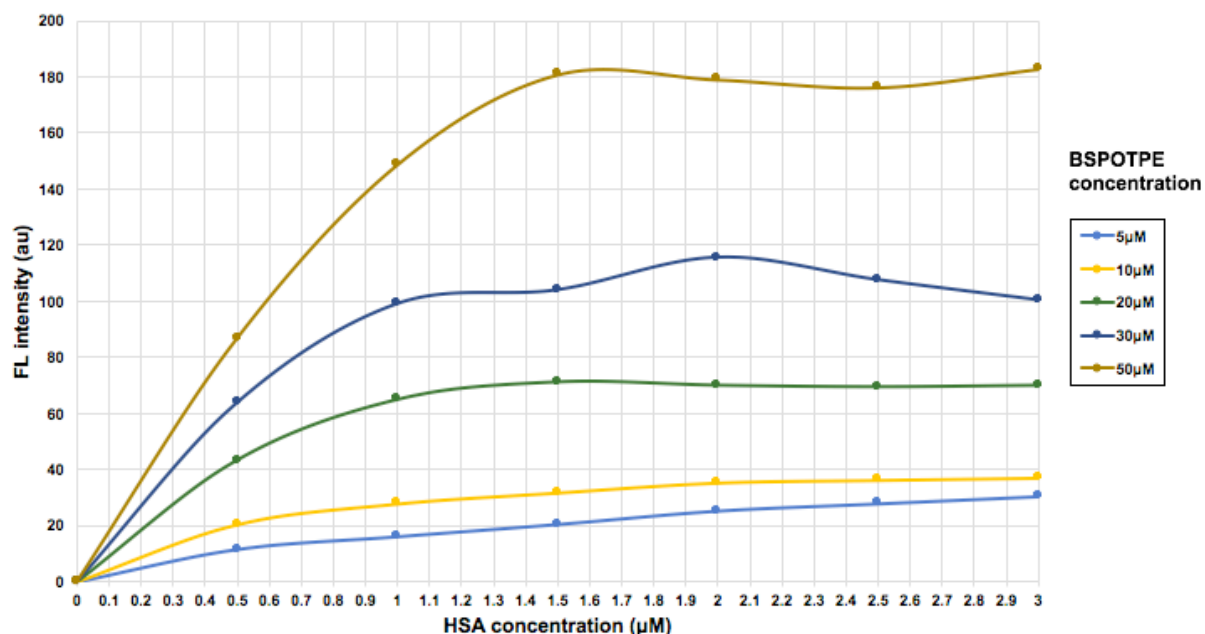


Figure 31. The change in the fluorescent light intensity with different HSA concentrations by applying different BSPOTPE concentrations. BSPOTPE=300 $\mu$ L, HSA=2700 $\mu$ L.

#### 4.1.4 Incubation time

The time of the interaction between BSPOTPE and HSA was another crucial factor. The time must be long enough for reaction to be complete[18]. Therefore, it was necessary to test the incubation time for BSPOTPE binding HSA. The value of light intensity and the accuracy of detection result were associated with the incubation time spent. The incubation time also determined the test time which should be reasonable for a fast test strip method. HSA with 1.5 $\mu$ M in urine sample of 2700 $\mu$ L was incubated in the presence of BSPOTPE solution with 50 $\mu$ M, 300 $\mu$ L before spectral measurement. The fluorescent light intensity was detected under different incubation time from 1 to 30 minutes. The result showed that the compound of BSPOTPE and HSA was turned on the light emission after an amount of time. The light intensity continuously increased with incubation time increasing but became almost constant at over 8 minutes. It illustrated that the binding reaction had finished approximately at 8 minutes. Therefore, it was better to take at least 8 minutes to obtain the maximized light intensity value, which could benefit the sensitivity and accuracy of the assay.

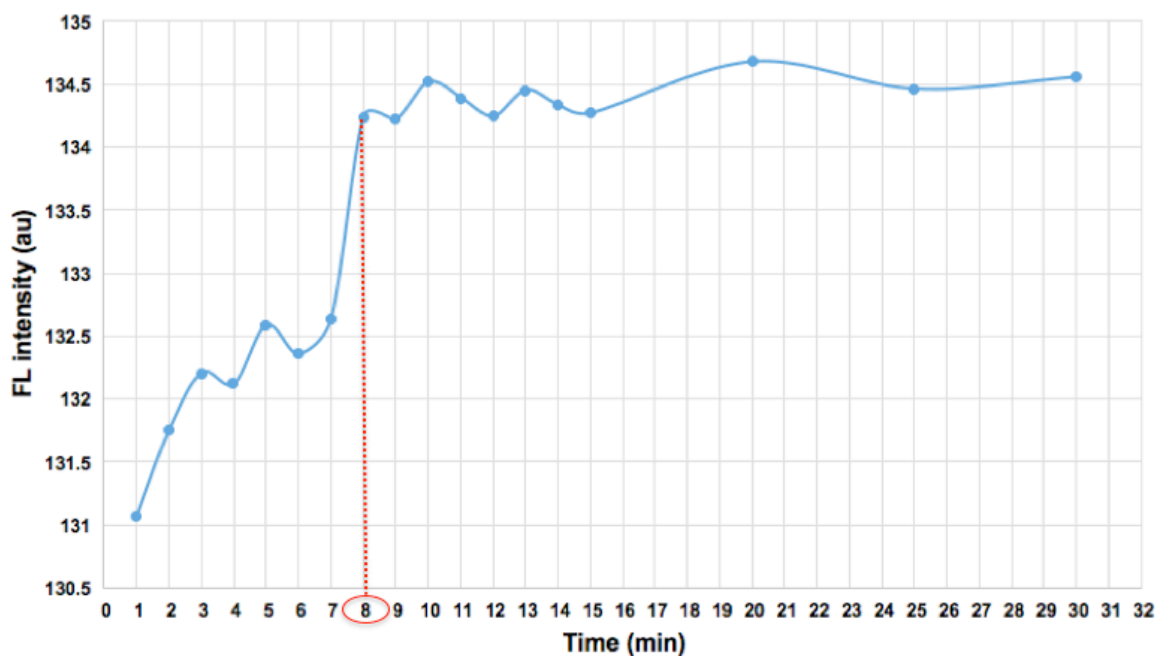


Figure 32. Incubation time examination. [BSPOTPE]=50 $\mu$ M, 300 $\mu$ L, [HSA]= 1.5 $\mu$ M, 2700 $\mu$ L.



### 4.1.5 Dipping time

We continuously improved the strip design. It was important to consider the time consuming during the test. The incubation time of BSPOTPE with albumin was investigated under the solution state. However, there might be a difference by conducting test strip under the solid state. As we introduced in the first chapter, BSPOTPE as AIEgen had the nature of aggregation-induced emission. It performed prominently under high concentration and solid state. In terms of strip based on dip method, the time for immersing into the sample and the time for waiting to detect after extracting were examined.

The strip pad was made of Fusion4 and dispensed with 50 $\mu$ M BSPOTPE. The urine samples with an HSA concentration of 0 $\mu$ M and 1.5 $\mu$ M were prepared by dissolving in an appropriate amount of artificial urine. Afterwards, immersing the strips by varying dipping time from 10 seconds to 900 seconds (15 minutes). The result demonstrated that the light intensity declined continuously whether or not albumin presence. The rate of the intensity reduction was fast at shorter dipping time and became almost constant at 60 seconds. Under the same dipping time, the higher albumin concentration the sample had, the smaller final intensity value was. This was probably caused by BSPOTPE dissolution rate in the urine sample. The rate was fast in the presence of albumin in the sample, which resulted from high selectivity of BSPOTPE toward albumin. If a mass of albumin existed in the sample, the BSPOTPE adhered to the strip pad would be attracted and bonded with the albumin in solution. The light intensity of the strip pad decreased after BSPOTPE had moved to the liquid sample. The HSA concentration determined the dissolution rate of BSPOTPE and the quantity of BSPOTPE remained on the strip pad. In this assay, we chose 10 seconds as dipping time in order to obtain sufficient light signal and achieve better test sensitivity. However, the dipping time was difficult to control in actual operation. Even if one-second difference occurred, the final light intensity would vary significantly, which might lead to a weak accuracy of the test strip.

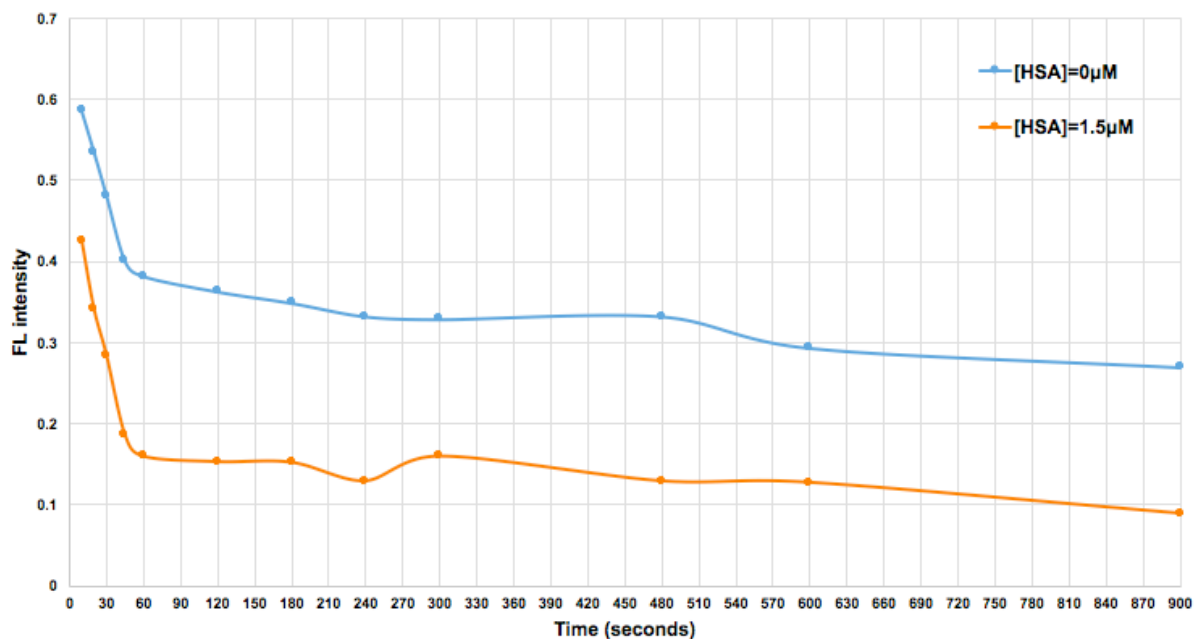


Figure 33. Dipping time examination by applying different HSA concentration. [BSPOTPE]=50μM, 50μL, [HSA]=3mL.

#### 4.1.6 Waiting time

After the strip was extracted from the urine sample, we should determine when the strip could be taken the picture. An appropriate waiting time was tested to ensure the strip pad had enough reaction time and obtained the best signal. We employed Fusion4 as optimized glass fiber which made the strip pad. The pad, which was mounted with BSPOTPE concentration of 50μM, was immersed into the urine sample of 3mL with HSA concentration of 1.5μM. The dipping time was set to 10 seconds. After taking out the strip, we tested the image intensity by time increasing from 3 minutes to 150 minutes under the room temperature. Figure 34 depicted that the strip fluorescent light intensity kept rising by time increasing. The intensity value entered into stability after waiting two hours, while the strip color appeared apparently. This test demonstrated that when the strip was wet, the light intensity of the pad was weak. The best time to take an image of the strip was after two hours. At that time, the strip pad was totally dry and its fluorescent light intensity could achieve the highest value. The reason might be that the property of BSPOTPE was aggregation-induced emission. This type of fluorogen was characterized by the light emission under the



high concentration or solid state. The solid state could serve more brightness comparing with liquid state. However, the strip test had to wait at least two hours under the room temperature to be dry. In the respect of waiting time, it took too long time to the test.

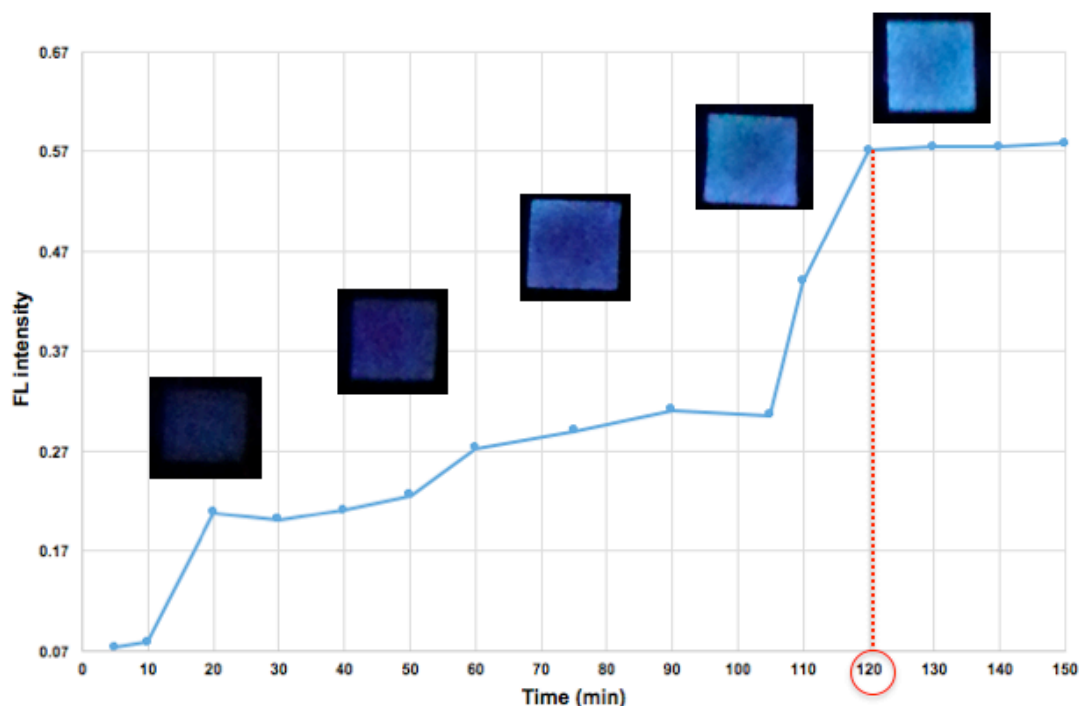


Figure 34. Waiting time examination. [BSPOTPE]=50 $\mu$ M, 50 $\mu$ L, [HSA]= 1.5 $\mu$ M, 3mL.

#### 4.1.7 Result

The test strip based on dip method utilized optimized conditions to perform the detection of HSA concentration. The strip pad, which was the conjugate pad as well as the result presenting area, was made of Fusion4 glass fiber with the size of 10mm $\times$ 10mm. The BSPOTPE of 50 $\mu$ M concentration was mounted on the pad. The strip was dipped into the urine sample in 10 seconds then taken out. After 2 hours waiting, the strip was totally dry and ready to be detected. We prepared urine samples with different HSA concentrations from 0.1-3 $\mu$ M. The image of strip pad was processed by Matlab code and the value of fluorescent light intensity was analyzed by plotting a graph.

We plotted the intensity value against the concentration of HSA and obtained a calibration curve by fitting to data using a Microsoft Excel program. The equation for

the calibration curve and the correlation of coefficient (R) were carried out as well. The values were nonlinear and a polynomial fitting curve was formed using multiple regression assay in Excel. The LINEST function could be employed to find the best fit curve for these nonlinear data. For the polynomial equation, the Excel did that by applying array constants and a second-degree polynomial was obtained to best fit the data. The R, which was known as the coefficient of multiple determination for multiple regression, was a statistical measure for how close the data was to the fitted regression curve. The higher the R, the better the equation fit the data.

In dip assay system, the polynomial fitting curve was plotted by fluorescent light intensity value at the y-axis against the albumin concentration at the x-axis. We observed the equation of  $y=0.0492x^2-0.2131x+0.5484$ , and R of 0.729. The intensity value for fitting calibration curve was obtained as the average of 3 independent strips at each albumin concentration. The assay maintained low reproducibility (standard deviation of the results was over 20%). This meant the precision of the assay performed poorly.

The calibration curve was made between 0.1 and 3  $\mu\text{M}$ . The higher the concentration of HSA in the urine sample, the less light intensity of the compound on the strip pad. Therefore, the fluorescent light intensity at the pad was inversely related to the amount of HSA in the urine sample. The reason we discussed before might be that as HSA concentration increasing, the BSPOTPE on the pad was captured increasingly by albumin in the sample and its dissolution rate kept rising. The more BSPOTPE moved out of the strip pad, the less light intensity left on the image. Figure 35 indicated that the intensity value changed considerably at lower albumin concentration ( $<1\mu\text{M}$ ) in the samples. As the albumin concentration in the samples increased, the slope of decreased intensity was reduced. The variation of light intensity approximately remained unchangeable after  $2\mu\text{M}$ . This finding explained that this strip design had excellent sensitivity in lower albumin level detection ( $<2\mu\text{M}$ ).

The test strip based on dip assay had low precision due to its large variation of individual analytical performance. To achieve a rich signal image, it had to conduct at least 2 hours. The equation of the calibration curve had the R-value of 0.729 which

was not high. The performance of this equation might not represent well for the actual value detection. However, this approach allowed low HSA concentration (<2 $\mu$ M) detection with prominent sensitivity. While the strip had this advantage, it was still inappropriate since it required time-consuming procedures and possessed low precision evaluation.

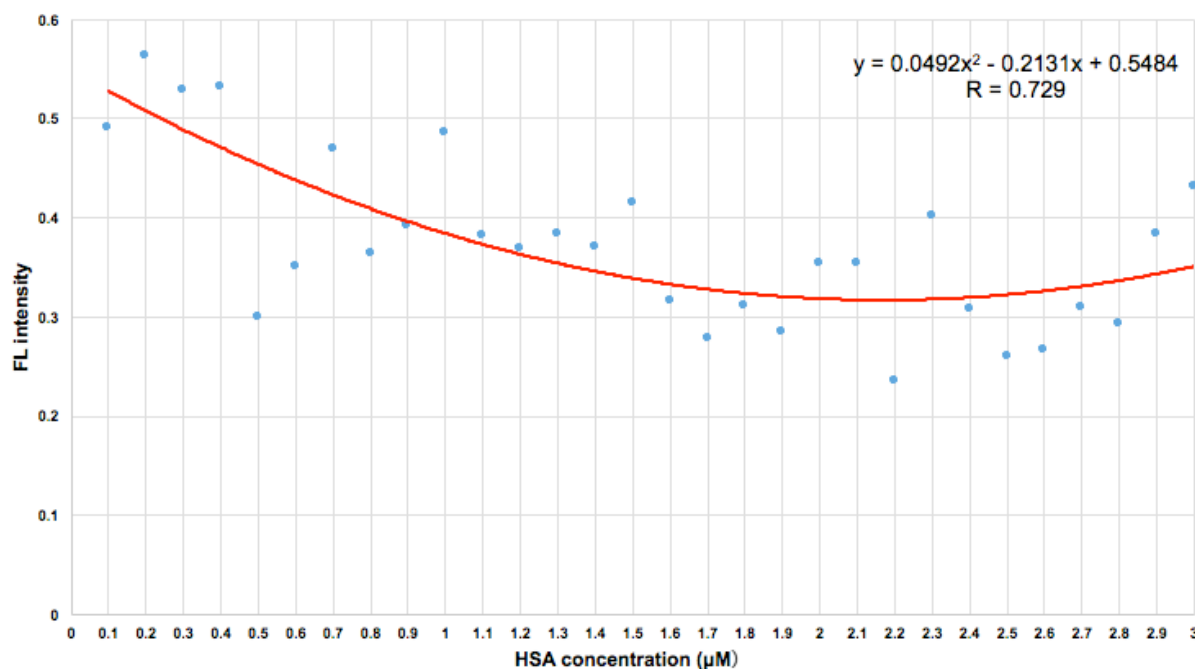


Figure 35. The plot of fluorescent light intensity against HSA concentration by applying dip strip.

## 4.2 Strip based on drop method

### 4.2.1 Strip design

The strip based on drop method was composed of three parts which included conjugate pad, reaction membrane and absorbent pad. The materials of glass fiber, NC membrane, and wicking paper were employed to make each component, respectively. The conjugate pad, where the sample was dropped, was mounted by BSPOTPE with 50 $\mu$ M, 50 $\mu$ L. The reaction membrane was the place to bind the target compound and to show the fluorescent light intensity result. The absorbent pad disposed of remaining fluid sample. Assembling of all components onto a plastic backing after dispensing of BSPOTPE at the conjugate pad. The dimension of each component was 10mm $\times$ 10mm. When the urine sample dropped onto the conjugate pad, the fluid met BSPOTPE and flowed to NC membrane where the compound of

BSPOTPE and HSA was captured and immobilized. The compound emitted fluorescent light and waited to be detected. The sample residue was absorbed by the last component. After waiting for a period of time to support incubation time, a picture of reaction membrane which exhibited abundant signal intensity was analyzed by image processing.

Unlike the strip design based on dip method, this design utilized NC membrane instead of glass fiber to become reaction area as well as the image taken place. The material replacement could improve the homogeneity and resolution of the image due to the difference of material structure characteristics. The chromatographic design took advantage of different materials' properties to assure the sample flow homogeneously through each component of the strip. In general, test strips were able to absorb only a fraction of a milliliter of a urine sample. Increasing the volume of urine sample applied in the lateral flow test did not considerably influence the accuracy of the test. Future improvement of the accuracy could be achieved only by optimizing the test conditions not by increasing the sample volume[18]. In this test, the immunoassay was unused. There were no test line and control line in the reaction membrane. However, a promising strategy was to combine the lateral flow assay and the colorimetric method. The luminescent compound in the reaction membrane could be detected and it represented the concentration of the target analyte.

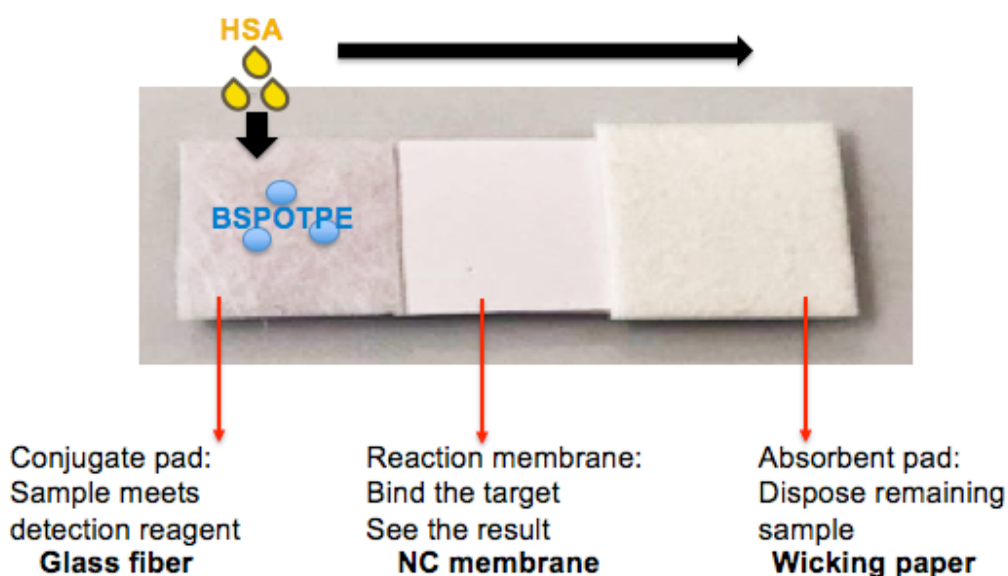


Figure 36. Strip base on drop method

## 4.2.2 Nitrocellulose membrane (NC membrane)

NC membrane as a reaction area as well as result showing place was utilized in drop method. Membranes were available in different grades which were highly important in determining the sensitivity of the test. An excellent membrane should support good binding to capture albumin with BSPOTPE. The membrane could offer high affinity for proteins. The wicking rate of the membrane could affect the test sensitivity and was determinant by membrane porosity. We purchased two popular types of NC membranes for selection: Sartorius CN140 and Sartorius CN95. The membrane morphologies and the uniformities of pore distribution across the membrane were investigated by SEM.

The appearance of two NC membrane surface was white, flat and smooth. The membrane had a clean and defect-free surface. Both membranes were casted directly onto a 100 $\mu$ m transparent polyester film which acted as a back support. The backed polymers were hydrophobic. Not just for supporting, the backing also worked as a barrier against card glue. The membrane had the characteristic of immediate and long-term uniform wettability after fluid flowing. This feature allowed a clear and uniform signal reading at the end of the test.



Figure 37. The appearance of original NC membrane under the visual light.

(A) CN140 (B) CN95

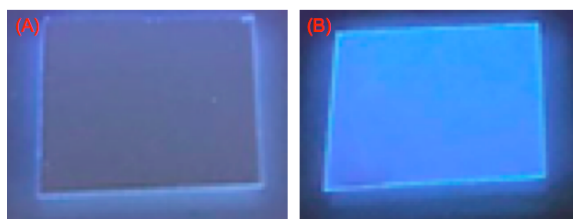


Figure 38. CN140 shows uniform wettability under 365nm UV light.

(A) Before wetting (B) After wetting

Under the SEM, we examined the structure of two NC membranes. The result described that the membrane was highly porous and its 3D structure was like a sponge. The defined pore structure of these membranes yielded a controlled wicking rate of samples.

CN140 had a relatively small and close pore structure compared with CN95, which was around  $8\mu\text{m}$ [45]. It exhibited a tremendous inner surface area which concentrated detection complex to generate a readable signal area. CN95 had a very large pore size of  $10\mu\text{m}$ [45]. This open structure was particularly adapted for running on viscous or particle loaded samples, such as colloidal gold. The membrane pore size was determinant of the wicking rate. Larger pore size contributed to a faster wicking rate. CN95 had much larger pore size than CN140. Hence, CN95 had a much faster wicking speed.

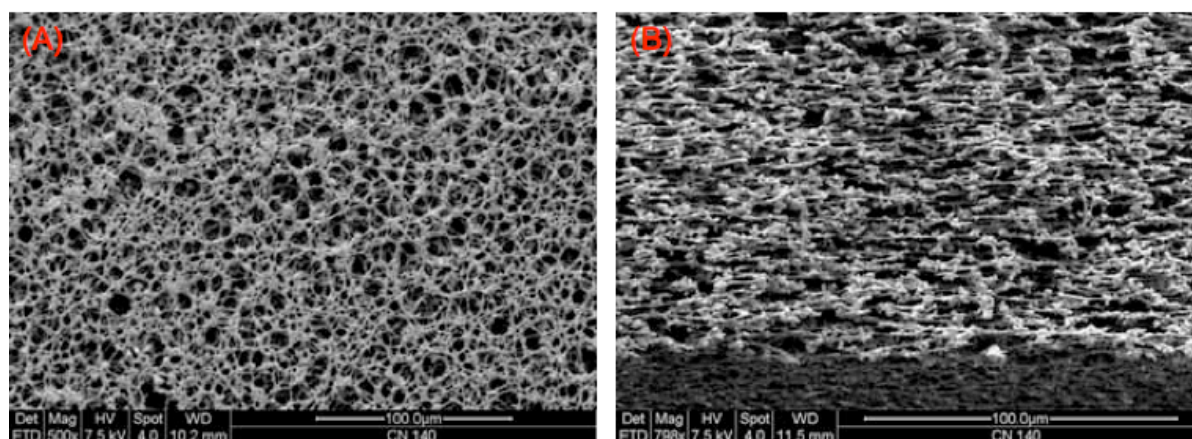


Figure 39. CN140 under the SEM[45].

(A) Air side (SEM@500X; bar= $100\mu\text{m}$ ) (B) Cross section (SEM@440X; bar= $100\mu\text{m}$ )

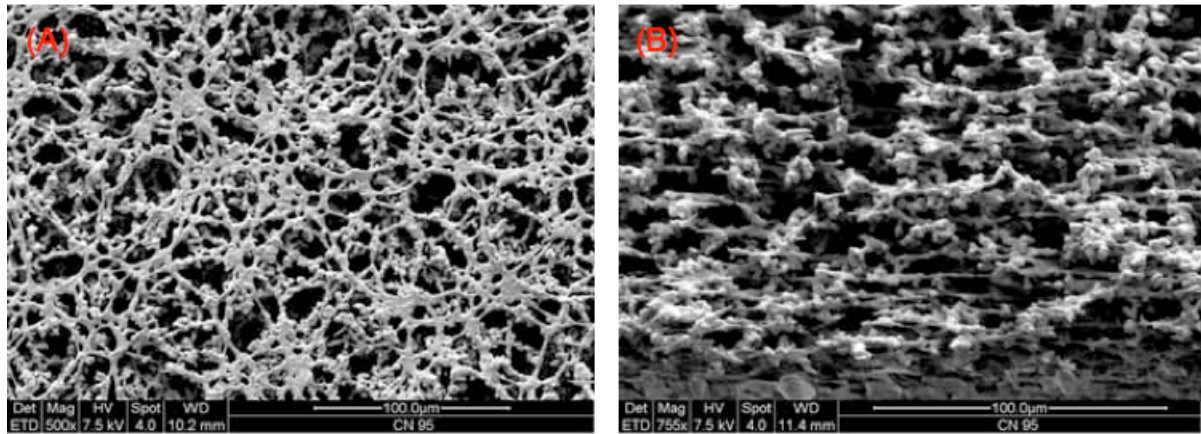


Figure 40. CN95 under the SEM[45].

(A) Air side (SEM@500X; bar=100µm) (B) Cross section (SEM@800X; bar=100µm)

The prepared affinity membranes were used to capture protein. Due to their high inner surface area, membranes contributed to protein binding capacity per membrane area. When fluid laterally flowed over the membranes, numerous affinity proteins were immobilized onto the membranes. The slower wicking speed of the membrane, the more proteins binding in the porosity structure. More protein captured on the membrane, higher signal intensity obtained. Consequently, the test result achieved a better sensitivity.

Due to the shorter time of capillary rise, CN95's spread rate was too fast to obtain a sensitive signal intensity value. It generated a shorter time to signal on the membrane and was suitable for the test not required high-level sensitivity. The use of NC membrane with slow wicking rate could improve specific interaction and gave a lower detection limit[18]. CN140 membrane could capture more proteins and be better for this assay which required slower wicking speed for higher sensitivity.



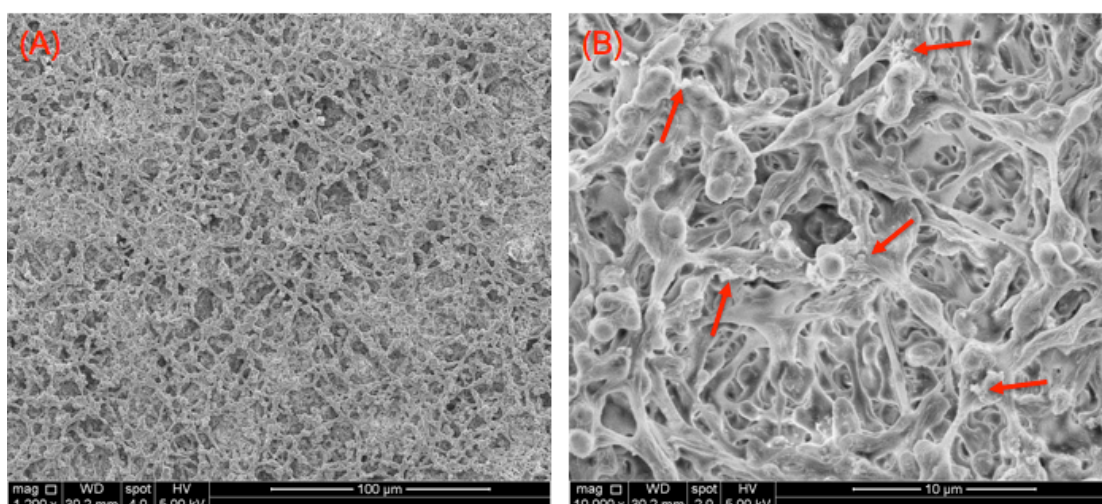


Figure 41. CN140 with complex of BSPOTPE and HSA

(A) SEM@1200X, bar=100 $\mu$ m (B) SEM@1000X, bar=10 $\mu$ m

NC membrane with its unique microporous property became essential for the development of quantitative assay in a drop test. Membranes presented high non-specific binding of proteins because of the particular electrostatic and hydrophobic surface feature. Proper dispensing of the fluorescent compound, drying and blocking played a crucial role in improvement of assay's sensitivity[19]. In this experiment, an appropriate membrane should be characterized by fine pore which would result in a slower wicking rate. Then more complex of HSA and BSPOTPE could be captured by the membrane. CN140 with smaller pore size had excellent protein sorption ability contributing to a high sensitivity of the test. CN90 with very open pore structure had a fast time to signal but weak ability to immobilize protein, which lead to lower sensitivity.

NC membrane name	Thickness ( $\mu$ m) (membrane layer)	Capillary speed (s/40mm)	Nominal pore size ( $\mu$ m)	Protein binding ( $\mu$ g/cm <sup>2</sup> )
<b>CN140</b>	125-155	110-165	8	30
<b>CN95</b>	140-170	90-135	10	28

Table 3. Critical parameters of membranes[45].



### 4.2.3 Glass fiber

In the design of strip based on dip method, we had investigated and optimized the glass fiber as conjugate pad as well as reaction pad. For strip design based on drop method, the criteria of glass fiber selection were similar: the more BSPOTPE coated, the better. Apart from high load capability of reagent, the glass fiber should have the capability to transfer BSPOTPE to reaction membrane. We monitored transferring capability of Fusion4 and Ahlstrom8964 as the conjugate pad when applying urine samples with different HSA concentrations of  $0.3\mu\text{M}$  and  $3\mu\text{M}$ . The test utilized optimized conditions such as 8-minute reaction time and using CN140 as NC membrane. The conjugate pad, which was mounted with BSPOTPE ( $50\mu\text{M}$ ), pushed fluorogens and sample to reaction membrane. As we could see from Figure 42, Fusion4 enabled BSPOTPE moving to next component successfully whether HSA concentration was  $0.3$  or  $3\mu\text{M}$  and the membrane exhibited fluorescent light. Ahlstrom8964 could only transfer fluorogens with  $0.3\mu\text{M}$  HSA, but difficultly carried fluorogens to the membrane when HSA concentration was  $3\mu\text{M}$ . We could see light intensity accumulated at the boundary of glass fiber and NC membrane. The membrane was in the absence of fluorescent light. Hence, it was better to select Fusion4 as the conjugate pad on account of excellent BSPOTPE carrying and transferring capability.

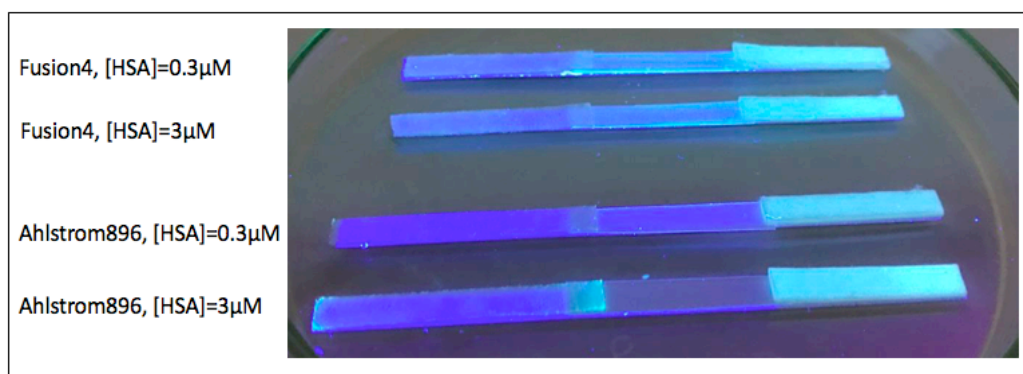


Figure 42. The transferring capability comparison of two glass fibers under different HSA concentrations. [BSPOTPE]= $50\mu\text{M}$ ,  $50\mu\text{L}$ , HSA=  $50\mu\text{L}$ .

#### 4.2.4 Testing time

Although the incubation time was tested and showed the sufficient reaction time was at least 8 minutes under the solution state, we investigated an appropriate testing time of strip which was designed by the drop assay. The test applied Fusion4 and CN140 to make conjugate pad and reaction membrane, respectively. The strip was coated by BSPOTPE with optimized concentration of 50 $\mu$ M and waited to encounter samples with or without HSA. The sample dropped onto the strip and flowed through each component. Afterwards, the time commenced accumulating. The image of reaction zone was captured after waiting 1 to 30 minutes. The result depicted that the fluorescent light intensity decreased regardless of the HSA concentration. The BSPOTPE was feebly luminescent in the absence of HSA. When a small amount of HSA was added, the BSPOTPE became luminescent obviously and constantly. It was clear to observe that the light intensity magnitude of the sample with 1.5 $\mu$ M HSA was much larger than the sample without HSA. The intensity of sample without HSA dropped considerably with further time increase. In contrast, the sample having HSA kept stable at the first few minutes and slightly decreased.

The reason for light intensity decrease might be the capillary action of the absorbent pad which was adjacent to the reaction membrane. Most of the fluid was absorbed and stored by the last pad. It was inevitable that some number of luminescent albumin moved to absorbent pad accompanying by the fluid. The NC membrane had the characteristic of excellent protein adsorption capability. If the sample was in the absence of HSA, the BSPOTPE would hardly immobilize on the membrane. Almost all BSPOTPE migrated to the last pad and no light intensity on the NC membrane. Whereas, if the sample had a certain amount of HSA, the HSA could bind BSPOTPE together and be captured by NC membrane. A large amount of albumin complex was immobilized on the membrane and kept emitting fluorescent light. As a result, the curve of the light intensity could sustain constantly with large intensity value. Although the intensity value declined moderately due to the capillarity, we still could use it to detect HSA concentration with prominent accuracy.

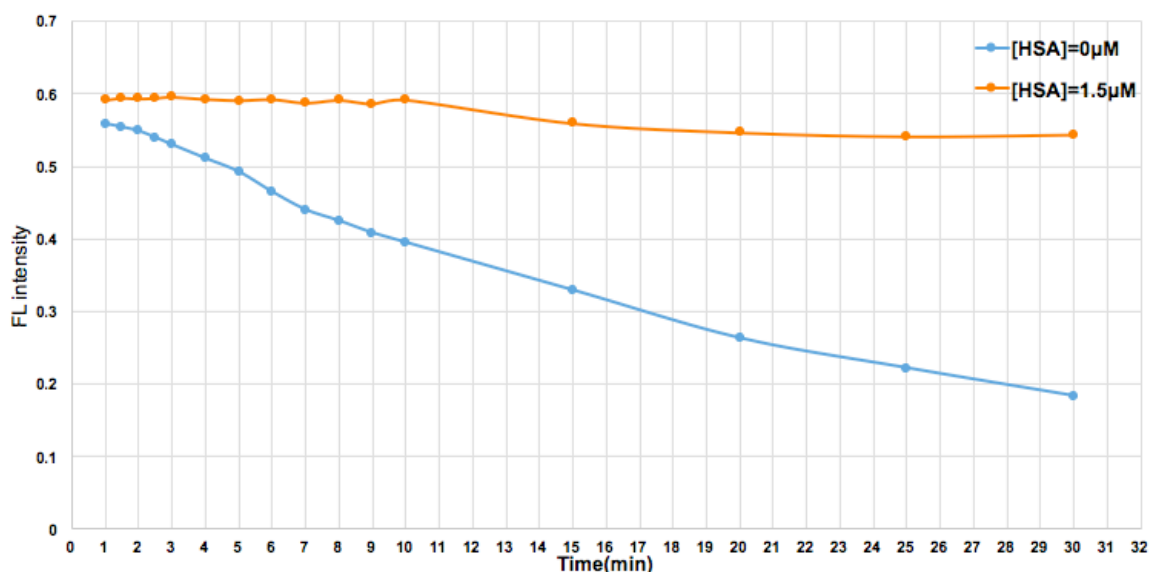


Figure 43. Testing time examination by applying different HSA concentrations. [BSPOTPE]=50 μM, 50 μL, [HSA]= 50 μL.

As waiting time increased, the light intensity of the membrane decreased slightly for a sample having HSA. To examine when the appropriate testing time was, we observed the curve in detail. The curve of 1.5 μM HSA sample remained stable at first 10 minutes. Afterwards, it dropped quickly because of absorbent pad absorption. This feature might arise from protein absorption of NC membrane. In the first 10 minutes, luminescent albumin was grasped rapidly by the membrane. The amount of protein largely reduced in the fluid, which resulted in wicking speed rise. Consequently, the membrane capture time reduced, which lead to light intensity fell slightly and accessed to the second stable stage. This feature supported to determine the strip testing time. Although the last pad would finish absorbing fluid after 25 minutes and the light intensity entered into stability again, the intensity value of second stable stage was too small to serve test sensitivity. Therefore, the experiment chose to take an image within 10 minutes in order to receive high light intensity value.

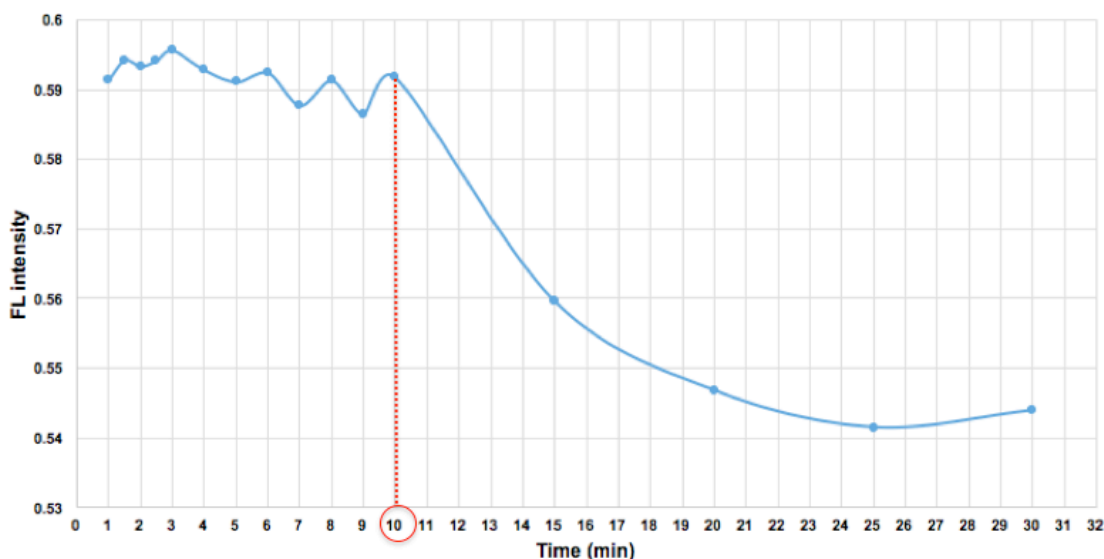


Figure 44. Appropriate testing time examination. [BSPOTPE]=50 $\mu$ M, 50 $\mu$ L, [HSA]= 50 $\mu$ L.

#### 4.2.5 Result

The design of test strip used drop assay employed optimal materials and conditions to monitor HSA concentration in the urine sample. It had three components: the conjugate pad, reaction membrane, and absorbent pad, which were made of Fusion4 glass fiber, Sartorius CN140 NC membrane, and wicking paper, respectively. Each component was a dimension of 10mm $\times$ 10mm and assembled sequentially onto the backing support which was a hydrophobic laminate polystyrene card. The BSPOTPE with 50 $\mu$ M concentration was immobilized on the conjugate pad. After dropping 50 $\mu$ L of urine samples on this pad, the fluid flowed through each component. The membrane presented the light signal. We took an image from the membrane within 10 minutes. Using image processing, we converted the fluorescent light signal into the intensity value. The results were plotted in Figure 45 for analyzing.

A calibration curve was displayed throughout the entire measuring range from 0.1 to 3 $\mu$ M. A polynomial fitting curve and its equation of  $y=0.0061x^2-0.0047x+0.6035$  were shown. We obtained a strong correlation of coefficient ( $R=0.868$ ) between albumin concentration and test strip reflectance data, which meant the equation represented well to fit given data. During the test, the value for fitting the curve was the mean of 3 replicate strips at each albumin concentration. Due to the standard

deviation of light intensity value was within 10-20%, the precision seldom achieved the satisfied value (<10%) but was improved a lot comparing with dip assay.

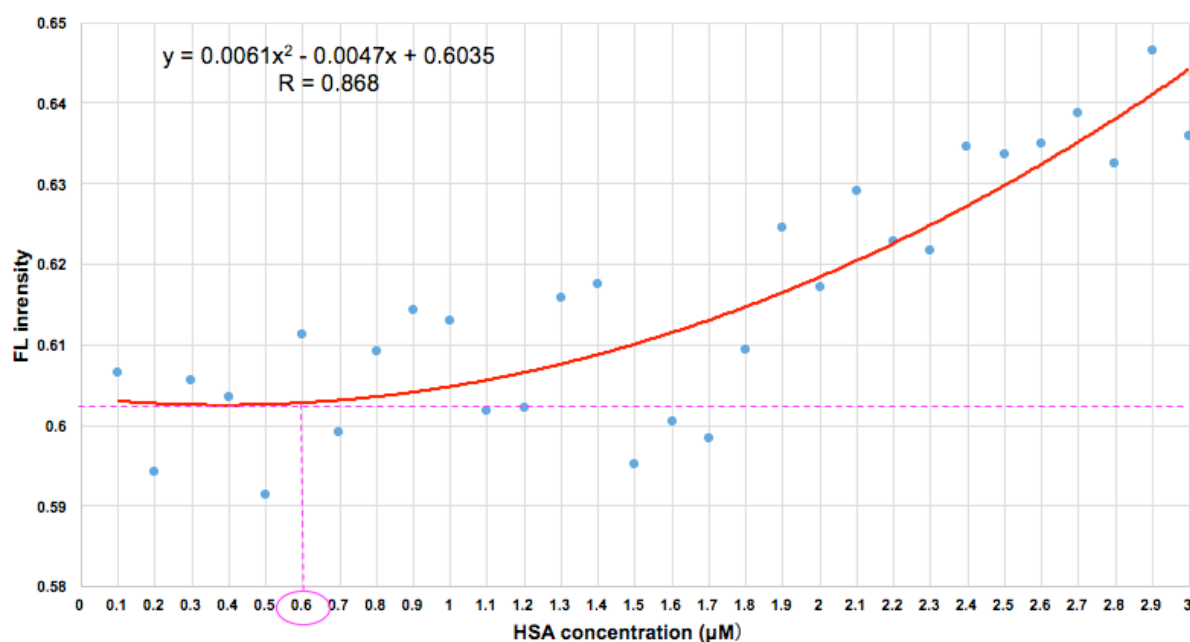


Figure 45. The plot of fluorescent light intensity against HSA concentration by applying drop strip.

We observed the feature of the plotted fitting curve. The fluorescent light intensity increased steadily by HSA concentration increasing. The more luminescent albumin captured by NC membrane, the higher light intensity obtained. However, the curve presented invariance at lower concentration of HSA ( $<0.6\mu\text{M}$ ). As the albumin concentration increased after  $0.6\mu\text{M}$ , the slope of the intensity value rose significantly, especially over  $2\mu\text{M}$ . This feature demonstrated that this strip design was appropriate for measuring high albumin concentration ( $>0.6\mu\text{M}$ ) because of high sensitivity.

To summarize this drop assay, the strip exhibited a good correlation between the light intensity and the albumin concentration ( $R=0.868$ ). The high value of  $R$  represented reasonable reliability in this assay system. It was sensitive to monitor higher albumin concentration ( $>0.6\mu\text{M}$ ) with better precision. The reproducibility of the method was good. However, the detection limit was  $0.6\mu\text{M}$  and the detection range of this assay was  $0.6-3\mu\text{M}$ . The micro-albuminuria for early detection kidney disease was  $30-300\text{mg/L}$  ( $0.45-4.5\mu\text{M}$ ). Our design focused on  $30-150\text{mg/L}$  ( $0.45-2.26\mu\text{M}$ ) because the detection limit of conventional urine test strip was  $150\text{mg/L}$  ( $2.26\mu\text{M}$ ), which covered the concentration of  $150-300\text{mg/L}$  ( $2.26-4.5\mu\text{M}$ ). Therefore, there was

a detection gap of the concentration (0.45-0.6 $\mu$ M) for micro-albuminuria analysis by performing this design, but it was still an acceptable measurement.

## **4.3 Method comparison**

### **4.3.1 Dip and drop assay comparison**

In the present study, we tried to explore the feasibility of advanced urine test strip based on AIEgen bioprobe technology for obtaining quantitative micro-albuminuria test results. We constructed two assay systems to quantify the albumin concentration: strip based on dip method and strip based on drop method.

For quantitative methods, there was a high requirement for accuracy. The correlation coefficients of two models for micro-albuminuria detection in dip test and drop test were 0.729 and 0.868, respectively. Due to the higher R-value and smaller standard deviation, the drop assay showed a better performance over a wide concentration range. The reflectance of the dip strip test was easily affected. We found that its light intensity values of the repeated tests fluctuated considerably, which resulted in lower precision. For the drop assay, in addition to its reliable analytical performance, it could be completed in 10 minutes without any pretreatment. In contrast, the dip assay consumed at least 2 hours to receive the results.

From Figure 46, the calibration curve of the drop test relatively expressed smaller variation range of the intensity value as evidenced by the smaller slope comparing to the dip test, especially the slope in the low-level range was less steep than that of the dip test. This might lead to less sensitivity if the evaluation code was not good enough. We observed the dip pattern that even though the variation range in light intensity was not very noticeable at the albumin concentration of over 2 $\mu$ M in the samples, it implemented excellently under 2 $\mu$ M. Due to this feature, the dip pattern could easily measure the clinically important threshold value of 0.45 $\mu$ M. Conversely, the detection range of drop pattern was 0.6-3 $\mu$ M and it was hard to monitor HSA concentration smaller than 0.6 $\mu$ M.

In conclusion, both designs might make the conduct of BSPOTPE assay feasible, especially utilize the drop methodology.

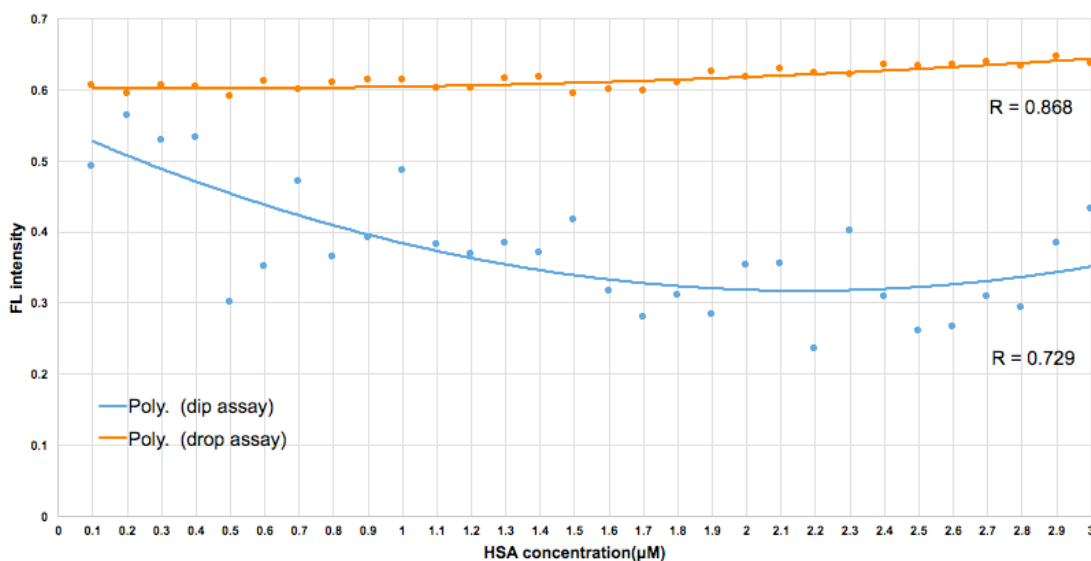


Figure 46. Comparison of the test strip based on dip and drop method

### 4.3.2 Traditional urine test strip comparison

Traditionally, for the test strip assay, the albumin concentration could be measured by utilizing dye-binding and immunological methods. The dye-binding method was mostly based on tetrabromophenol blue, which was a semi-quantitative colorimetric method. The detection limit of this method was 150mg/L (2.26μM) and it was much larger than the micro-albuminuria minimum value of 30mg/L (0.45μM). Furthermore, the color difference was analyzed through human eyes, which might cause a false result. Our design could allow quantitative determination of micro-albuminuria over a very wide albumin concentration range (drop assay: 0.6-3μM, dip assay: <2μM). These results were remarkable in particular when taking into account that the quality of existing dye-binding albuminuria assay was sometimes disappointed. In contrast to the subjective analysis by human eyes, there was less risk for analytical errors due to the use of image processing procedure.

One major difference between our strip design and the conventional fluorescent immunochromatographic assay (FICA) was that AIEGen as fluorescent dye was employed to detect the analyte. The traditional fluorescence dye (organic fluorophore or QDs) had no selectivity to albumin, therefore it needed to bind with antibody for reaction. It also had the characteristic of ACQ effect which lead to the false result under a high analyte concentration. Due to its design based on immunoassay, FICA

strip was produced in a complicated process and cost a lot. In contrast to our design, the high cost of evaluation machine for FICA also made it less suitable for convenient mass screening, in particular in developing countries. Our new test strip based on AIEgen had high selectivity to HSA. There was no antibody binding and no quenching occurred under high concentration. It was analyzed by smartphone and MATLAB code, which was portable and easy-going. The new design simplified the strip configuration and reduced the production cost.

In this study, we discussed the potential of strip test based on AIEgen technology as an affordable and convenient alternative for micro-albuminuria test. These results demonstrated that the new AIEgen strip assay supported the feasibility of CKD early detection and could be further developed in future research.

#### **4.4 Limitations of the research**

Some limitations of the design were addressed here such as restriction of raw materials, absence of solid fluorescence reader, and inability of image improvement. In our study, we chose two types in each material. The glass fiber and NC membrane were selected in a small range according to the previous study experience. This limited the possibility of precision and accuracy improvement. We were absent of two machines. One was an inkjet printer for BSPOTPE immobilization on NC membrane. The BSPOTPE coated on NC membrane might lead to better result instead of mounting on glass fiber. This strategy would substantially reduce the required volumes of BSPOTPE as detection reagent for the test, which would significantly lower the cost per test[18]. Another machine was a fluorescence spectrophotometer for detecting actual value of solid fluorescence. It could help us to confirm the reliability of the fluorescent light intensity under solid state. In addition, for the image processing analysis, there was a lack of effective method of image quality enhancement to improve the homogeneity of the images by software. If the design could break these limitations, the performance of the strip would be significantly improved.



## 4.5 Future directions of further advance study

### 4.5.1 Combination with immunoassay

As far as precise quantification is required, the immunological method is conventionally regarded as a good choice among the analytical assays. As technical progress in test strip detection has generated new possibilities for micro-albuminuria analysis, next study can combine the test strip based AIEgen assay with a classical immunological method.

In the traditional design of FICA strip, the fluorogen (QDs) doesn't have selectivity, so it has to label on one antibody, then the labeled antibody has the properties to target at the analyte as well as be lighted on. It needs three types of antibody to finish the entire design. Furthermore, the process of QDs production is toxic and complicated. But now, due to the property of AIEgen, only use itself can achieve two goals: high selectivity and light-on feature. In the next step, the strip can be modified like Figure 47. We can switch the labeled antibody to AIEgen on conjugate pad, then print one type of antibody at the test line on NC membrane for immobilizing the albumin defined as antigen, at last delete the secondary antibody. The new design only needs one antibody, and the production process is non-toxic and cost effective.

After dropping the sample, the albumin is bonded with BSPOTPE and the compound is highly captured by the test line due to the immunoreaction. Diagnostic accuracy of micro-albuminuria can be improved by this high specificity, which allows amounts of luminescent albumin to immobilize on the test line, increasing the light intensity of the image but eliminating the variable influence of the non-homogeneity. New assay development can be undertaken with more confidence, especially with regard to the development of high standard quantitative assays.

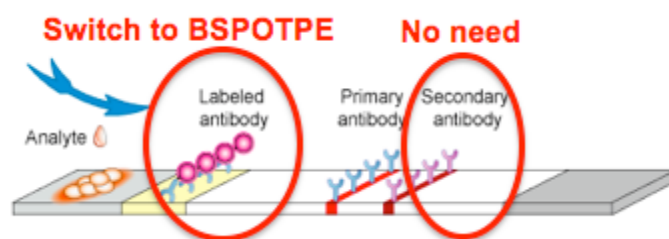


Figure 47. Test strip combined with immunoassay

## **4.5.2 Advanced material search**

Material selection of different physical parts is utilized to improve quantitation ability of the test strip. Improvement in materials can be beneficial in enhancing sensitivity and reproducibility of existing methods[18]. Search new materials which can provide multipurpose job can be helpful in achieving goals of high reproducibility and good sensitivity.

To find a new glass fiber owning high density of fibers may contribute to keeping more fluorogens around the surface of each fiber. More fluorogens mounted lead to a brighter image which has more abundant signal information. The NC membrane is highly critical. It performs as a main motor of the test. It draws the sample with conjugate reagent from one side of the strip to the other side. The urine sample-BSPOTPE complex can be immobilized by the membrane. New material serving well-distributed pore size can enhance affinity for HSA and support for controlling the flow of sample[19]. This may result in enough reaction time and more proteins immobilizing inside membrane's sponge structure. A new type of NC membrane with the characteristic of immediate and long term uniform wettability should be developed to offer the features essential for highly reproducible readouts. These reliable materials may enable test strip with excellent performance characteristics.

## **4.5.3 New strip configuration**

The traditional design of a lateral flow strip comprises four parts. However, our study deletes the first component: a sample pad. The sample pad is designed to pretreat the urine sample before its flow. This pretreatment may include separation of sample components, removal of interferences, and adjustment of pH, etc.[19]. The reason we do not apply sample pad is that our samples are prepared by artificial urine and our design does not include preliminary clean up steps. In actual urine, there are urine sediments and the pad can remove sediments from the sample. Hence, it is necessary to add it in actual urine diagnosis.

#### **4.5.4 Evaluation tool improvement**

The smartphone employed in the future study should have an excellent camera sensor. This camera sensor can provide high resolution, reproducible images, and a wide dynamic range of light intensity for measurement[18]. The MATLAB code also has an opportunity for further improvement and calibration. Since a smartphone-based point-of-care urinalysis device, which is based on AIEgen detection under the solution state, has already been developed by Shaymaa's research, it is still necessary to design a detection device based on strip test due to its hygiene and convenience[13]. The future work includes a design of the strip photographing accessory for the smartphone, which can provide a dark environment with 365nm UV light. This accessory enables micro-albuminuria detection anywhere at anytime by using our AIEgen strip. It will combine with a smartphone application for image analysis as well. All images and analyzed data will upload to the cloud for telemedicine, then the patient and doctor can diagnose and supervise the albumin level conveniently.

# Chapter 5: Conclusions

This study conducts a feasibility design of urine test strip for early detection of chronic kidney disease. The strips which are based on AIEgen bioprobe BSPOTPE are designed by two different methodologies: dip and drop assay. Both designs optimize their component materials and test conditions. The strip based on the dip method obtains an equation between fluorescent light intensity and albumin concentration with a low R-value and a high standard deviation, which means that its precision and accuracy are weak. However, it has good sensitivity of albumin concentration detection under  $2\mu\text{M}$ . The strip based on the drop method implements well due to excellent equation performance but its detection range of albumin is  $0.6\text{-}3\mu\text{M}$  which does not cover the micro-albuminuria. Both strip designs can perform albumin detection with different detection ranges. However, the performance of strip applying the drop methodology is better than that of the dip methodology.

Our study contributes to the optimization of raw materials and test conditions when designing the strip with AIEgen. We provide the design criteria of AIEgen based strip and build two prediction models through fitting curves of the experiment results. These contributions can support the strip design in the next stage. It is better to combine immunoassay for accuracy improvement of the strip based on drop assay. Advanced material search, new strip configuration, and evaluation tool improvement should be further investigated in future research. This feasibility study demonstrates that a smartphone-based urinalysis by using AIEgen based test strip for early detection of chronic kidney disease has the opportunity to be commercially available.

# Appendixes

## Appendix 1: Conference collection

The thesis results have been collected by 13<sup>th</sup> Chinese Chemical Society National Conference on Analytical Chemistry. The abstract of research is presented as following.

### **Aggregation-induced emission fluorogen based urine test strip for early detection of chronic kidney disease**

Xinyi Zhang <sup>1</sup>, Anh Tran Tam Pham <sup>1</sup>, Youhong Tang <sup>1,\*</sup>

<sup>1</sup> College of Science and Engineering, Flinders University, South Australia 5042, Australia

\*Email : [youhong.tang@flinders.edu.au](mailto:youhong.tang@flinders.edu.au)

Early detection of chronic kidney disease (CKD) can reduce the kidney failure by up to 50 percent. Micro-albuminuria, which means the protein concentration is 30-300 mg/L, is an indicator of CKD in early stage. A few of in-vitro diagnostic devices base on fluorescent emission to assay the chronic kidney disease have been developed, such as the strip test, which always combines a device for quantitative analysis. In this study, we try to use a specified designed AIEgen to substitute the expensive, tedious-prepared and ACQ effecting quantum dot fluorogen labelled antibody and the corresponding antigen in the current test strip and redevelop the medical device to achieve a more cost-effective with acceptable detection ability in-vitro diagnostic system for own healthcare management. The individual parts of the strip, such as sample pad, conjugate pad, NC membrane and the assembled strip using the optimised individuals have been evaluated.

**Key words:** aggregation-induced emission, chronic kidney disease, urine test strip

## Appendix 2: MATLAB code

The MATLAB code for urine albumin test strip based on AIEgen bioprobe is provided by Shaymaa Akraa and Ravichandran Rasiyah[13]. Here is a code example for HSA concentration detection using strip based on drop methodology.

```
Concen = {0.1 0.2 0.3 0.4 0.5 0.6 0.7 0.8 0.9 1.0 1.1 1.2 1.3 1.4 1.5 1.6 1.7
1.8 1.9 2.0 2.1 2.2 2.3 2.4 2.5 2.6 2.7 2.8 2.9 3.0};
numcon = length(Concen);

X = cell (1, numcon);

for k = 1: numcon

X{k} = Concen{k};

end

myimages = {'0.1.jpg'; '0.2.jpg'; '0.3.jpg'; '0.4.jpg'; '0.5.jpg'; '0.6.jpg';
'0.7.jpg'; '0.8.jpg'; '0.9.jpg'; '1.0.jpg'; '1.1.jpg'; '1.2.jpg'; '1.3.jpg';
'1.4.jpg'; '1.5.jpg'; '1.6.jpg'; '1.7.jpg'; '1.8.jpg'; '1.9.jpg';
'2.0.jpg'; '2.1.jpg'; '2.2.jpg'; '2.3.jpg'; '2.4.jpg'; '2.5.jpg'; '2.6.jpg';
'2.7.jpg'; '2.8.jpg'; '2.9.jpg'; '3.0.jpg'};

numbering = length(myimages);

X2 = cell (1, numbering);

image1 = cell (1, numbering);
%X1 = {[200,1000,200,200],200,1200,200,200}, [200,1600,100,100]];
%order of the crop is top, middle, bottom

for k = 1: numbering
image1{k} = imread(myimages{k});
X2{k} = imcrop(image1{k}, [1,1,1000,1000]);
figure,
imshow(X2{k});
end

R = cell(1,numbering);

G = cell(1,numbering);
```

```

B = cell(1,numbering);

H = cell(1,numbering);

S = cell(1,numbering);

I = cell(1,numbering);

mI = cell(1,numbering);

Y = cell(1,numbering);

for k = 1:numbering

%figure;

%imshow(X2{k});

%Represent the RGB image in [0 1] range

X2{k}=double(X2{k})/255;

R{k}=X2{k}(:,:,1);

G{k}=X2{k}(:,:,2);

B{k}=X2{k}(:,:,3);

%Hue

numi=1/2*((R{k}-G{k})+(R{k}-B{k}));

denom=((R{k}-G{k}).^2+((R{k}-B{k}).*(G{k}-B{k}))).^0.5;

%To avoid divide by zero exception add a small number in the denominator

H{k}=acosd(numi./(denom+0.000001));

%If B>G then H= 360-Theta

H{k}(B{k}>G{k})=360-H{k}(B{k}>G{k});

%Normalize to the range [0 1]

```

```

H{k}=H{k}/360;

%Saturation

S{k}=1- (3./(sum(X2{k},3)+0.000001)).*min(X2{k},[],3);

%Intensity

I{k}=sum(X2{k},3)./3;

mI{k} = mean2(I{k});

%display(mI{k});

Y{k} = mI{k};

end

%display(X, 'Concentration');
%display(Y, 'Mean Intensity');
Z1 = cell2mat(X); % convert cell to number
Z2 = cell2mat(Y);
%figure('units','normalized','outerposition',[0 0 1 1])
%plot(Z1,Z2,'b');
%Z2 = cell2mat(Y);
%hold on;
%P = polyfit(Z1,Z2,3);
figure,
plot(Z1, Z2,'o');%5legend('top', 'middle', 'bottom');
%plot(P);
%legendtext = [legendtext; num2str(A(k)), 'Location', 'Best']
%hold all;
%Z2 = cell2mat(Y);
%hold on;
%plot(Z1, Z2,'o');
title('HSA Concentration Vs FL Intensity')
xlabel('HSA Concentration(uM)')
ylabel('FL Intensity')

```



# References

1. Jha, V., et al., *Chronic kidney disease: global dimension and perspectives*. The Lancet, 2013. **382**(9888): p. 260-272.
2. Levey, A.S. and J. Coresh, *Chronic kidney disease*. The lancet, 2012. **379**(9811): p. 165-180.
3. Stevens, P.E. and A. Levin, *Evaluation and management of chronic kidney disease: synopsis of the kidney disease: improving global outcomes 2012 clinical practice guideline*. Annals of internal medicine, 2013. **158**(11): p. 825-830.
4. Hong, Y., et al., *Quantitation, visualization, and monitoring of conformational transitions of human serum albumin by a tetraphenylethene derivative with aggregation-induced emission characteristics*. Analytical chemistry, 2010. **82**(16): p. 7035-7043.
5. Martin, H., *Laboratory measurement of urine albumin and urine total protein in screening for proteinuria in chronic kidney disease*. The Clinical Biochemist Reviews, 2011. **32**(2): p. 97.
6. Parikh, C.R., *A point-of-care device for acute kidney injury: a fantastic, futuristic, or frivolous 'measure'?* Kidney international, 2009. **76**(1): p. 8-10.
7. Liu, R., et al., *Methodological evaluation and comparison of five urinary albumin measurements*. Journal of clinical laboratory analysis, 2011. **25**(5): p. 324-329.
8. Chen, T., et al., *Quantitative urinalysis using aggregation-induced emission bioprobes for monitoring chronic kidney disease*. Faraday discussions, 2017. **196**: p. 351-362.
9. Xie, H., et al., *An AIE-based fluorescent test strip for the portable detection of gaseous phosgene*. Chemical Communications, 2017. **53**(70): p. 9813-9816.
10. Hong, Y., J.W. Lam, and B.Z. Tang, *Aggregation-induced emission: phenomenon, mechanism and applications*. Chemical communications, 2009(29): p. 4332-4353.
11. Hong, Y., J.W. Lam, and B.Z. Tang, *Aggregation-induced emission*. Chemical Society Reviews, 2011. **40**(11): p. 5361-5388.
12. Ding, D., et al., *Bioprobes based on AIE fluorogens*. Accounts of chemical research, 2013. **46**(11): p. 2441-2453.
13. Akraa, S., et al., *A smartphone-based point-of-care quantitative urinalysis device for chronic kidney disease patients*. Journal of Network and Computer Applications, 2018.
14. Delanghe, J.R., et al., *Sensitive albuminuria analysis using dye-binding based test strips*. Clinica Chimica Acta, 2017.
15. Barratt, J. and P. Topham, *Urine proteomics: the present and future of measuring urinary protein components in disease*. Canadian Medical Association Journal, 2007. **177**(4): p. 361-368.

16. Meyer, N.L., et al., *Urinary dipstick protein: a poor predictor of absent or severe proteinuria*. American journal of obstetrics and gynecology, 1994. **170**(1): p. 137-141.
17. Choi, S., et al., *A rapid, simple measurement of human albumin in whole blood using a fluorescence immunoassay (I)*. Clinica Chimica Acta, 2004. **339**(1): p. 147-156.
18. Dzantiev, B.B., et al., *Immunochemical methods in food analysis*. TrAC Trends in Analytical Chemistry, 2014. **55**: p. 81-93.
19. Sajid, M., A.-N. Kawde, and M. Daud, *Designs, formats and applications of lateral flow assay: A literature review*. Journal of Saudi Chemical Society, 2015. **19**(6): p. 689-705.
20. Meurant, G., *Immunoassay: A practical guide*. 2012: Elsevier.
21. Gao, M. and B.Z. Tang, *Fluorescent Sensors Based on Aggregation-Induced Emission: Recent Advances and Perspectives*. ACS sensors, 2017.
22. Tong, H., et al., *Protein detection and quantitation by tetraphenylethene-based fluorescent probes with aggregation-induced emission characteristics*. The Journal of Physical Chemistry B, 2007. **111**(40): p. 11817-11823.
23. Qiu, Z., et al., *A Simple and Sensitive Method for an Important Physical Parameter: Reliable Measurement of Glass Transition Temperature by AIEgens*. Macromolecules, 2017. **50**(19): p. 7620-7627.
24. Jiang, G., et al., *Fluorescent turn-on sensing of bacterial lipopolysaccharide in artificial urine sample with sensitivity down to nanomolar by tetraphenylethylene based aggregation induced emission molecule*. Biosensors and Bioelectronics, 2016. **85**: p. 62-67.
25. Chutipongtanate, S. and V. Thongboonkerd, *Systematic comparisons of artificial urine formulas for in vitro cellular study*. Analytical biochemistry, 2010. **402**(1): p. 110-112.
26. Qu, H., et al., *Rapid lateral-flow immunoassay for the quantum dot-based detection of puerarin*. Biosensors and Bioelectronics, 2016. **81**: p. 358-362.
27. Ruckenstein, E. and W. Guo, *Cellulose and glass fiber affinity membranes for the chromatographic separation of biomolecules*. Biotechnology progress, 2004. **20**(1): p. 13-25.
28. Fang, C., et al., *Smartphone app-based/portable sensor for the detection of fluoro-surfactant PFOA*. Chemosphere, 2018. **191**: p. 381-388.
29. Hou, Y., et al., *Smartphone-Based Dual-Modality Imaging System for Quantitative Detection of Color or Fluorescent Lateral Flow Immunochemical Strips*. Nanoscale Research Letters, 2017. **12**(1): p. 291.
30. Cisbio 2016, *Testosterone radioimmunoassay kit*, viewed 1 May 2018, <<https://www.cisbio.com/other/diagnostics/products/endocrinology/testosterone-radioimmunoassay-kit>>.
31. Rapolu, C 2013, *Radioimmunoassay*, SlideShare, 17 July, viewed 1 May 2018, <<https://www.slideshare.net/chakravarthyrapolu/radio-immuno-assay>>.

32. ThermoFisher 2018, *Human Serum Albumin Human ELISA Kit*, viewed 1 May 2018, < <https://www.thermofisher.com/order/catalog/product/EHALB>>.
33. ELISA Technologies 2017, *Laboratory Equipment*, viewed 1 May 2018, < <https://www.elisa-tek.com/laboratory-equipment/>>.
34. Microzones 2013, *Urine Test Strips*, viewed 1 May 2018, < <http://microzones.co.za/product/urine-test-strips/>>.
35. ALCO-Safe 2018, *Concateno Drug Screen Test - Single Drug Cassette Tests*, viewed 1 May 2018, < <http://www.alcosafe.co.za/Products/Drug-Testing-Urine/Single-Drug-Cassette-Tests>>.
36. Cheng, X., et al., *Rapid and quantitative detection of C-reactive protein using quantum dots and immunochromatographic test strips*. *International journal of nanomedicine*, 2014. **9**: p. 5619.
37. Chen, S., et al., *Fabrication of fluorescent nanoparticles based on AIE luminogens (AIE dots) and their applications in bioimaging*. *Materials Horizons*, 2016. **3**(4): p. 283-293.
38. Medical World 2015, *CLINITEK STATUS CONTROL STRIPS X 25*, viewed 1 May 2018, < <https://www.medical-world.co.uk/p/urine-analysis/siemens/bayer-clinitек-urine-analyser/clinitек-status-control-strips-x-25/17019>>
39. medical supermarket 2018, *Combur Urine Test Strips*, viewed 1 May 2018, < <http://www.medical-supermarket.com/Shop/ProductPage.aspx?productID=61587>>.
40. Ronald J., et al. 2010, *Proteinuria*, Wayback Machine, 29 July, viewed 1 May 2018, <<https://emedicine.medscape.com/article/984289-overview>>.
41. Creative-Diagnostic 2009, *Immunochromatography Guide*, viewed 1 May 2018, < <https://www.creative-diagnostics.com/Immunochromatography-guide.htm>>.
42. Drug Test Success 2018, *Mission Urinalysis Reagent Strips*, viewed 1 May 2018, <<https://www.drugtestsuccess.com/supplies/mission-urinalysis-reagent-strips>>
43. All Test 2018, *4mm 300ng Quick Drug Abuse Test Kit COC Urine Drug Test Strip / Cassette / Panel*, viewed 1 May 2018, < <http://www.custom-monoclonalantibody.com/sale-3565913-4mm-300ng-quick-drug-abuse-test-kit-coc-urine-drug-test-strip-cassette-panel.html>>.
44. Joey-bio 2018, *Conjugate pad glass fiber filter paper Ahlstrom 8964*, viewed 1 May 2018, < [http://www.joey-bio.cn/product/60500517788-800533937/Conjugate\\_pad\\_glass\\_fiber\\_filter\\_paper\\_Ahlstrom\\_8964.html](http://www.joey-bio.cn/product/60500517788-800533937/Conjugate_pad_glass_fiber_filter_paper_Ahlstrom_8964.html)>.
45. Sartorius 2018, *UniSart® Nitrocellulose Membranes: The Substrate of Choice for Protein Assays*, viewed 1 May 2018, <[https://www.sartorius.com/mediafile/Broch\\_UniSart\\_Nitro\\_SL-1536-e.pdf](https://www.sartorius.com/mediafile/Broch_UniSart_Nitro_SL-1536-e.pdf)>.